THE FATE OF PHENOLIC COMPOUNDS IN THE AMERICAN LOBSTER, *HOMARUS AMERICANUS*

BY

CHUNG-LI JASON LI

A DISSERTATION PRESENTED TO THE GRADUATE SCHOOL
OF THE UNIVERSITY OF FLORIDA IN PARTIAL FULFILLMENT
OF THE REQUIREMENTS FOR THE DEGREE OF
DOCTOR OF PHILOSOPHY

UNIVERSITY OF FLORIDA

1993

To My Father

Chin-Chung Li

and My Mother

Shiu-Fong Yang

To My Wife

Chi-Yin Gina Wu

and My Daughter

Catherine Y.F. Li

ACKNOWLEDGEMENTS

I would like to express my sincere appreciation to my advisor, Dr. Margaret O. James, for providing me with the opportunity to study with her. Her scientific guidance and inspiration were essential to the production of this project.

I would also like to thank Dr. Mace G. Barron for his invaluable discussions on pharmacokinetics and Dr. Kenneth Sloan for his technical assistance with IR spectrophotometer and NMR spectrometer. A special thanks goes to Dr. Dan Weiner for his assistance with the pharmacokinetic modeling.

Lastly, my gratitude is extended to Mr. Sean M. Boyle, graduate student, Mr. Allen Altman, technician, and staff of the Department of Medicinal Chemistry, College of Pharmacy for their assistance and friendship which helped my study in University of Florida to be enjoyable and productive.

TABLE OF CONTENTS

LIST OF TABLES

LIST OF FIGURES

Abstract of Dissertation Presented to the Graduate School of the University of Florida in Partial Fulfillment of the Requirements for the Degree of Doctor of Philosophy

THE FATE OF PHENOLIC COMPOUNDS IN THE AMERICAN LOBSTER, *HOMARUS AMERICANUS*

By

Chung-Li Jason Li

August, 1993

Chairman: Margaret O. James
Major Department: Medicinal Chemistry

Although lobsters are known to metabolize lipophilic organic compounds by monooxygenation, little is known of the fate of the hydroxylated metabolites. Studies were designed to determine the ability of lobster tissues to conjugate phenolic compounds and how they were eliminated from the animal. Aryl sulfotransferase (ST) activity was present in the cytosolic fraction of the antennal gland (AG), but not hepatopancreas (HP), whereas UDP-glucosyltransferase (UDPGT) activity was found in microsomal fractions of both AG and HP. The ß-naphthol UDPGT exhibited different pH optima in HP (10.5) and AG (7.5) microsomes, suggesting that more than one form of ß-naphthol UDPGT exists in the lobster. Single doses of [^{14}C]-phenol, 0.019 to 2.8 mg/kg, and [^{14}C]-ß-naphthol, 0.25 mg/kg, were administered intrapericardially to groups of lobsters. Phenol concentrations decreased rapidly in

hemolymph (α $t_{1/2}$ = 8.74 ± 0.02 min; ß $t_{1/2}$ = 14.00 ± 0.03 min) and part of the dose was excreted through gills into tank water as parent phenol in the first 30 minutes. The phenol that was not excreted through gills was rapidly conjugated to phenyl sulfate. This sulfate conjugate was slowly ($t_{1/2}$ 6.3 to 11.9 h) eliminated from the hemolymph through the AG into urine. The fate of phenol in the lobster was controlled by two competing processes, namely, excretion of parent compound across the gills and biotransformation in the AG to phenyl sulfate which was slowly excreted in urine. The contribution of each process was dose dependent. ß-Naphthol (α $t_{1/2}$= 26 ± 19 to 29 ± 15 min; ß $t_{1/2}$=30.6 ± 6.8 to 63.9 ± 30.9 h) was rapidly metabolized by two competing conjugating enzymes, ST and UDPGT, and the conjugates were slowly eliminated from the lobster. The minor metabolite, ß-naphthyl sulfate, ($t_{1/2}$ 7.8 to 9.4 h) was formed in the AG, excreted into urinary bladder, and eliminated from urine. The major metabolite, ß-naphthyl glucoside ($t_{1/2}$ 28.9 to 51.2 h) was formed in the HP and the AG, and slowly eliminated. Since the major difference between phenol and ß-naphthol was lipophilicity, these studies show that lipophilicity plays an important role in determining how phenolic compounds are metabolized by the lobster *in vivo*, both quantitatively and qualitatively.

CHAPTER 1
INTRODUCTION

Human and other organisms are constantly exposed in their environment to a variety of chemicals that are foreign to their bodies. These chemicals, or *xenobiotics*, can be of natural origin or they can be man-made. In general, the more lipophilic compounds are readily absorbed through the protecting membranes, for example, the human skin or the cell membrane of the prokaryote. Constant or even intermittent exposure to these lipophilic chemicals could result in their accumulation within the organisms, unless effective means of elimination are present. Fortunately, living organisms have developed a number of biochemical processes that biotransform lipophilic compounds to more hydrophilic metabolites which can be easily excreted from the body.

Drug Metabolizing Enzymes

It is evident that various metabolites formed from a specific foreign compound result from the action of several enzymes acting in concert. Drug metabolism reactions have been divided into categories: phase 1 (functionalization) and phase 2 (conjugative) reactions (Williams, 1959). Phase 1, or functionalization reactions, include oxidative, reductive and hydrolytic biotransformations. The purpose of these reactions

is to introduce a polar functional group to the xenobiotic molecule which can be achieved by direct introduction of the functional group (e.g. aromatic and aliphatic hydroxylation) or by modifying or "unmasking" existing functionalities (e.g. reduction of ketones and aldehydes to alcohols, hydrolysis of ester and amide to yield COOH, NH_2 and OH groups). While phase 1 reactions may not produce sufficiently hydrophilic or inactive metabolites, they generally tend to provide a functional group or "handle" in the molecule that can undergo subsequent phase 2 reactions (Low and Castagnoli, 1982).

The purpose of phase 2 reaction is to attach small, polar and ionizable endogenous compounds such as glucuronic acid and sulfate to the functional "handle" of phase 1 metabolites to form water-soluble conjugated products. Parent compounds that already have existing functional groups are directly conjugated by phase 2 enzymes. Conjugated metabolites are readily excreted in the urine and are generally devoid of pharmacological activity and toxicity. It is apparent that phase 1 and phase 2 reactions complement each other in detoxifying and facilitating the elimination of drugs and xenobiotics (Low and Castagnoli, 1982).

Since both phase 1 and phase 2 enzymes convert foreign chemicals to forms that can be readily excreted, they are often referred to as *detoxication enzymes*. However, it should be emphasized that biotransformation is not strictly related to detoxication. In a number of cases, the metabolic products

are more toxic than the parent compounds. The term *toxication* or *bioactivation* is often used to indicate the enzymatic formation of reactive intermediates. These reactive intermediates are thought to initiate the events that ultimately result in cell death, chemically induced cancer, teratogenesis and a number of other toxicities. For example, the ubiquitous environmental pollutant benzo[a]pyrene is bioactivated by cytochrome P450 and epoxide hydrolase to form the ultimate carcinogen (+)-anti-benzo[a]pyrene-7,8-diol-9,10-epoxide.

Phase 1 Enzyme Reactions

Phase 1 reactions introduce or uncover functional groups. These reactions may add functional groups by two oxidative enzyme systems: the cytochrome monooxygenase P450 system (which was previously referred to as the mixed-function oxidase [MFO] system) and FAD-monooxygenase, previously called the mixed-function amine oxidase. Both enzyme systems introduce oxygen into the foreign substrate.

Preexisting functional groups are exposed by a family of hydrolytic enzymes, esterases and amidases. The cleavage of the ester or amide bond, regardless of the remaining chemical structure, will produce two functional groups for further biotransformation, a carboxylic acid plus either an amine (from an amide), or an alcohol (from an ester). Another hydrolase enzyme, epoxide hydrolase, adds water to an epoxide-containing xenobiotic and produces two hydroxyl groups.

Finally, a variety of oxidation-reduction systems can be considered part of the phase 1 enzymes since these are redox enzymes and often alter the oxidation state of a carbon to allow it to be more readily excreted or biotransformed by the phase 2 enzymes. The principal enzymatic systems involved in this redox reaction are: alcohol dehydrogenase, aldehyde reductase, ketone reductase and a number of aldehyde dehydrogenases (Sipes and Gandolfi, 1991).

Cytochrome P450 enzyme system

The most important enzyme systems involved in phase 1 reactions are the cytochrome P450-containing monooxygenases which can be found in many forms of organisms. The cytochrome P450 system is actually a coupled enzyme system consisting of two enzymes: NADPH-cytochrome P450 reductase and a heme-containing enzyme, cytochrome P450. These enzymes have been considered to be embedded in the phospholipid matrix of the endoplasmic reticulum of the cell, but recent evidence suggests that the P450 proteins are only linked to the phospholipid membrane by one or two transmembrane peptide segments, leaving the active site in the cytoplasm (Brown and Black, 1989).

The cytochrome P450 is a heme-protein. The heme portion is an iron-containing porphyrin called protoporphyrin IX, while the protein portion is called the apoprotein (Figure 1-1). In humans, cytochrome P450 is found in high concentrations in the liver, the major organ involved in the metabolism

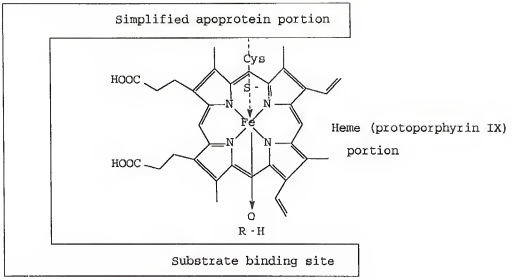

Figure 1-1. A simplified depiction of the proposed "activated oxygen"-cytochrome P450-substrate complex (Low and Castagnoli, 1982).

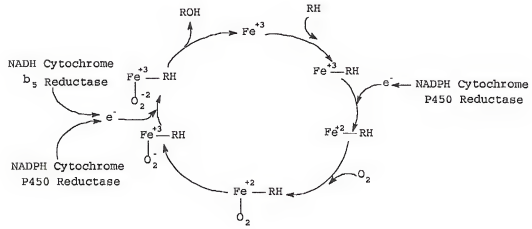

Figure 1-2. Catalytic cycle of cytochrome P450. RH represents the substrate and ROH the corresponding hydroxylated metabolite. (Adapted from White and Coon, Ann. Rev. Biochem., 49, 315-356, 1980).

of xenobiotics. It is also found in many other tissues (e.g. lung, kidney, placenta and skin), which indicates that these tissues have drug metabolizing capability too.

The name cytochrome P450 is derived from the fact that the reduced (Fe^{+2}) form of this enzyme binds with carbon monoxide to form a complex that has a distinguishing spectroscopic absorption maximum at 450 nm. The structure of the cytochrome P450 and mechanism of oxygen activation are reviewed by White and Coon (1980) and Black and Coon (1987). The mechanism of action for cytochrome P450 is outlined in Figure 1-2.

Cytochrome P450 enzyme systems can metabolize a number of endogenous compounds such as steroids, bile acids and biogenic amines. They also can metabolize a wide range of foreign chemicals including drugs, environmental pollutants and plant products. During 1985, less than a dozen cDNA and deduced protein sequences were available, but by 1990 more than 160 P450 genes had been characterized, ranging from 23 eukaryotes (including 9 mammalian and 1 plant species) to 6 prokaryotes (Nebert *et al.*, 1991). In our laboratory, we try to characterize cytochrome P450 systems in lobster species (James *et al.*, 1979; James and Little, 1980; James *et al.*, 1982; James, 1984; James, 1989c), purify the enzyme (James, 1990) and sequence the enzyme (ongoing research) in order to establish the structure and the evolutionary relationship of the lobster species with other species.

Phase 2 Enzyme Reactions

Phase 1 or functionalization reactions do not always produce hydrophilic or pharmacologically inactive metabolites. However, various phase 2 or conjugation reactions are capable of converting these metabolites to more polar and water-soluble products. Many conjugative enzymes accomplish this objective by attaching small, polar and ionizable endogenous molecules such as glucuronic acid, sulfate and glycine to the phase 1 metabolites or parent xenobiotic. The resulting conjugated products are relatively water-soluble and readily excretable. In addition, they generally are biologically inactive and nontoxic. Other phase 2 reactions such as methylation and acetylation do not generally increase water solubility but serve mainly to terminate or attenuate pharmacological activity (e.g. dopamine is methylated to 3-methyloxytyramine). The role of glutathione is to combine with chemically reactive compounds, which usually prevents damage to important biomacromolecules such as DNA, RNA and proteins. Thus, phase 2 conjugation reactions may usually be considered to be detoxifying pathways in drug metabolism, although there are exceptions (Low and Castagnoli, 1982). For example, sulfate conjugation of the 2-acetylaminofluorene (AAF) phase 1 metabolite, N-hydroxy-AAF, results in formation of a highly reactive, electrophilic N-O-sulfate ester which is mutagenic and carcinogenic (Lotlikar *et al.*, 1966).

There are some distinguishing features of most phase 2 reactions. First, the conjugating group (glucuronic acid, sulfate and methyl) is initially activated in the form of a coenzyme before transfer or attachment of the group. Second, there are appropriate transferases involved in transferring the group to accepting substrate.

Sulfate conjugates

For the hydroxyl group, an important conjugation reaction is sulfation. In humans, this reaction is catalyzed by the sulfotransferases, a group of soluble enzymes found primarily in liver, kidney, intestinal tract and lungs. Their primary function is to transfer inorganic sulfate to the hydroxyl group present on phenols and aliphatic alcohols. The resulting products are referred to as sulfate esters or ethereal sulfates. In addition, sulfation of aromatic amines and hydroxylamines to form the corresponding sulfamate and N-O-sulfate is occasionally seen.

The sulfate donor for these reactions is 3'-phosphoadenosine-5'-phosphosulfate (PAPS, Figure 1-3). This cofactor is synthesized from inorganic sulfate and ATP. Basically, there are two primary sources of inorganic sulfate: absorption of this anion from the gut and oxidation of the amino acid cysteine. Since the concentration of free cysteine is limited, an important determinant in the extent of sulfation of foreign chemicals is the availability of the cofactor, PAPS. The availability of dietary organic and

inorganic sulfates for PAPS synthesis was reviewed by Mulder (1981). Recently, Maziasz *et al.* (1991) and Rozman *et al.* (1992) provided more details on this topic.

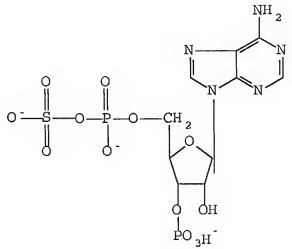

Figure 1-3. Structure of 3'-phosphoadenosine-5'-phosphosulfate (PAPS).

PAPS is synthesized from ATP and inorganic sulfate in sequential reactions catalyzed by ATP sulfurylase (EC 2.7.7.4) in Equation 1-1 and adenosine 5'-phosphosulfate (APS) kinase (EC 2.7.1.25) in Equation 1-2.

$$ATP + SO_4^{2-} \rightleftharpoons APS + PP \quad (1\text{-}1)$$

$$APS + ATP \rightleftharpoons PAPS + ADP \quad (1\text{-}2)$$

The sulfate activating system has been found in most mammalian tissues, and has been demonstrated in several invertebrates, crustaceans, mollusks and insects (Mulder, 1981

and 1990). Adenosine 3′,5′-diphosphate (PAP), a very potent inhibitor of the sulfotransferases (Falany *et al.*, 1990), is formed after transferring the sulfate group to the substrate.

There are four classes of sulfotransferases involved in detoxication processes. Aryl sulfotransferase conjugates phenols (EC 2.8.2.1), organic hydroxylamines (EC 2.8.2.3) and catecholamines (Banerjee and Roy, 1968; Foldes and Meek, 1973; Sekura and Jakoby, 1979; Sekura *et al.*, 1979; Anderson and Weinshilboum, 1980; Borchardt *et al.*, 1982; Campbell *et al.*, 1987; Heroux and Roth, 1988; Duffel *et al.*, 1989; Falany *et al.*, 1990; Johannes *et al.*, 1990; Neihrs and Huttner, 1990; Doolry *et al.*, 1991; Duffel *et al.*, 1991; Hirshey *et al.*, 1992). Phenol sulfotransferases from human liver cytosol consist of two distinct isoenzymes which are the monoamine- and phenol-sulfating phenol sulfotransferases. They are also referred to as the thermolabile and thermostable forms of phenol sulfotransferase (Falany, 1991).

Hydroxysteroid sulfotransferase conjugates hydroxysteroids and certain primary and secondary alcohols (Nose and Lipmann, 1958; Ogura *et al.*, 1990; Comer and Falany, 1992). Estrone sulfotransferase (EC 2.8.2.4) is active with phenolic groups on the aromatic ring of steroids (Hernandez *et al.*, 1992) and finally, bile salt sulfotransferases (EC 2.8.2.14) catalyzes the sulfation of both conjugated and unconjugated bile acids (Chen, 1982). The activities of these enzymes is

known to vary considerably with the sex and age of the animals.

After the sulfate conjugates have formed, they can be hydrolyzed by the sulfatases to parent compound or eliminated from the body in either the urine or bile. Generally speaking, there are two distinct types of aryl sulfatases (EC 3.1.6.1): those which are not inhibited by sulfate (type 1) and those which are (type 2). These enzymes were reviewed by Roy (1970). Kauffman *et al.* (1991) used isolated rat hepatocytes to study the futile cycling of sulfate conjugate formation and hydrolysis with the model compound 4-methylumbelliferone. Urinary and biliary excretions of sulfate conjugates were reviewed by Mulder (1981).

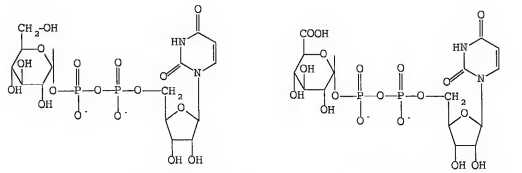

Figure 1-4. Structures of UDP-α-D-glucose and UDP-α-D-glucuronic acid.

Carbohydrate conjugates

Chemicals with phenolic hydroxy groups are substrates for both carbohydrate and sulfate conjugations. In vertebrates,

the preferred carbohydrate is UDP-glucuronic acid (UDPGA, Figure 1-4), while in the plants, insects and crustaceans the preferred co-substrate is UDP-glucose (UDPG, Figure 1-4), giving rise to glucosides (Dutton, 1980; James, 1987). But in the presence of UDPG, mice (Gessner et *al.*, 1973; Egestad and Sjöberg, 1992) and dog (Nakano et *al.*, 1986) liver microsomes can catalyze ß-glucosidation.

Common to all transferases, UDP-glycosyltransfeases also need co-substrate which can be either UDP-glucuronic acid or UDP-glucose depending on the species. UDPGA is a highly water-soluble, stable compound. It is formed inside the cell in a two-step reaction from glucose-1-phosphate and UTP. The first step is catalyzed by UDPG pyrophosphorylase (EC 2.7.7.9, Equation 1-3) to form UDPG. Subsequently, UDPG is oxidized at C_6 to UDPGA, which requires a four-electron oxidation in two steps (Equation 1-4). The activity of UDPG dehydrogenase (EC 1.1.1.22) is controlled by the NAD^+/NADH ratio (Mulder, 1990).

$$\text{Glucose-1-phosphate} + \text{UTP} \rightleftharpoons \text{UDPG} + \text{PPi} \qquad (1\text{-}3)$$

$$\text{UDPG} + 2\ \text{NAD}^+ \rightleftharpoons \text{UDPGA} + 2\ \text{NADH} + 2\ \text{H}^+ \qquad (1\text{-}4)$$

The mechanism of carbohydrate conjugation is a S_N2 reaction. The acceptor group of the substrate attacks the back side of the C_1 of the pyranose ring to which UDP is attached with an α-glycosidic bond. The resulting carbohydrate conjugate has the ß-glycosidic configuration. The attacking group should have sufficient nucleophilic

character for a high rate of carbohydrate conjugation. A wide variety of groups fulfil this requirement, such as phenols, carboxylic acids, thiophenols, alcohols, aromatic amines, hydroxylamines or hydroxamic acids. Even carbon atoms can attack C_1 of the pyranose ring if they are sufficiently nucleophilic, such as when carbon atoms are adjacent to two carbonyl groups (e.g. phenylbutazone), or ethynylic carbon atoms (e.g. ethinyl estradiol). The reactivity will depend on the electronic and steric factors of the compound. In some cases more than one group is available for conjugation, as in hyodeoxycholate, from which 3 glucuronides may be formed (Mulder, 1990). Normally conjugation with one of the functional groups is sufficient for excretion from the body.

The enzyme that carries out the reactions is either UDP-glucuronosyltransferase (EC 2.4.1.17) or UDP-glucosyl-transferase (EC 2.4.1.35). The enzyme activity is localized in the endoplasmic reticulum of numerous tissues, whereas most phase 2 enzymes are cytosolic enzymes. In humans, the liver, is quantitatively the most important tissue, but activity is also present in the kidney, intestine, skin, brain and spleen.

In vertebrates, the location of UDP-glucuronosyl-transferase in the microsomal membrane is physiologically important, since it may have direct access to the products formed by the action of microsomal cytochrome P450. Because there is remarkable latency of these enzyme activities in intact liver microsomes, it has been suggested that it is

necessary to transport the charged, membrane impermeable UDPGA across the microsomal membrane. However, no such evidence was found to support this hypothesis. Mechanical (freezing and thawing, sonication) or chemical (non-ionic detergent) disruption of the microsomes will activate the enzyme activity (Winsnes, 1972; Burchell and Coughtrie, 1989; Clarke *et al.*, 1991). Another hypothesis based on those observations is that the active center of the UDP-glucuronosyltransferase faces the cytosolic side of the microsomal membrane and the latency of the enzyme activities may reflect the presence of UDP-glucuronosyltransferase in a "constrained" conformational form (Vanstapel and Blanckaert, 1987).

There are several distinct forms of UDP-glucuronosyl-transferase. Enzyme heterogeneity explains in part (a) the differential increases in enzyme activities toward different aglycones following treatment with known microsomal enzyme inducing agents, (b) differential decreases in activities with respect to inhibition, and (c) species differences that lead to defects in glucuronidation of only certain classes of glucuronic acid acceptors.

The number of distinct forms of the enzyme is unknown at this time. A total of 26 distinct cDNAs in five mammalian species have been sequenced to date. Comparison of the deduced amino acid sequences leads to the definition of two families and a total of three subfamilies (Burchell *et al.*, 1991). There are at least three forms of UDP-

glucuronosyltransferases in rat liver microsomes. One isoenzyme exhibits a subunit molecular weight of 56,000 and is capable of conjugating *p*-nitrophenol, α-naphthol and 4-methylumbelliferone. This isoenzyme is inducible by 3-methylcholanthrene treatment and requires high UDPGA concentration for elution from the UDP-hexanolamine affinity column (Falany and Tephly, 1983).

Glucuronides are excreted from the body in either the bile or urine, depending on the size of the aglycone. In the rat, the kidney is the preferred route of excretion for aglycones with molecular weight less than 250 and bile is for aglycones with molecular weight more than 350. From 250 to 350 molecular weight, the conjugate may be excreted by either pathway. Molecular weight cutoffs for the preferred route of excretion vary with the animal species. In vertebrates, glucuronide conjugates are substrates for ß-glucuronidase (EC 3.2.1.31). There is considerable ß-glucuronidase activity present in the intestinal microflora which will release the aglycone back to the body and result in enterohepatic recirculation. Compounds involved in this cycle tend to have a longer half-life in the body and may undergo more extensive biotransformation before being eliminated (Sipes and Gandolfi, 1991). Much less is known about the enzymology, regulation and substrate selectivity of UDP-glucosyltransferase.

Sulfation seems to have a high affinity but low capacity for conjugation of phenols. Glucuronidation or glucosidation,

the major alternative reaction for phenols, has low affinity but a much higher capacity. Therefore, following administration of low doses of phenols, the major phenolic conjugate may be the sulfate ester. However, as the dose of phenol is increased, the percentage of dose converted to sulfate ester is decreased and carbohydrate conjugate will be dominant.

Pharmacokinetics

Pharmacokinetics is the study and characterization of the time course of drug absorption, distribution, metabolism and excretion, and the relationship of these processes to the intensity and time course of therapeutic and toxicologic effects of drugs (Gibaldi, 1991). Unlike a variety of behavioral, physiological and pharmacological responses, the principles of pharmacokinetics are described in terms of mathematical equations which are used to quantitatively predict the nature of these processes. The other term "*toxicokinetics*" is the modeling and mathematical description of the time course of disposition of xenobiotics in the whole organism (Klaassen and Rozman, 1991). From the definition of both terms, one can sense that the studies of toxicokinetics cover more chemicals than those of pharmacokinetics.

The process whereby a drug is made available to the fluids of distribution is referred to as absorption (Figure 1-5). The rate of this process depends on the method of administration, solubility and other physical properties of

the drug. Among all methods of administrative, intravenous injection has the shortest onset which allows the drug to reach the site of action very rapidly. There is much current interest in observations indicating that various preparations of the same drug administered orally may give different serum

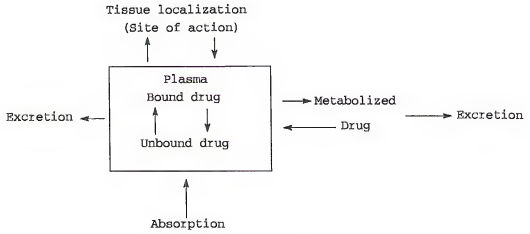

Figure 1-5. Absorption and fate of a drug (From Goth, 1981).

concentrations. The term *bioavailability* has been defined as the relative absorption efficiency of a test dosage form relative to a standard oral or intravenous preparation. After a particular route of administration, the area under the blood drug concentration-time curve (AUC) reflects the amount of drug that reaches the systemic sampling site. The ratio of AUC of a particular route of administration to $AUC_{intravenous}$ is a measure of the bioavailability of the drug after that particular route of administration (Goth, 1981).

Once a drug reaches the plasma, its main fluid of distribution, it must pass across various barriers to reach its final site of action by diffusion filtration. There are several factors that contribute to the unequal distribution of drugs in the body. Some of these are (1) binding to plasma proteins, (2) cellular binding, (3) concentration in body fat, and (4) the blood-brain barrier. Protein binding provides a depot, since the bound portion of the drug is in equilibrium with the free form. As the unbound fraction is excreted or metabolized, additional amounts are eluted from the protein. It also prolongs the half-life of a drug in the body, since the bound fraction is not filtered through the renal glomeruli and is not exposed to biotransformation until freed (Goth, 1981). The blood-brain barrier which is a protecting device for brain, spinal cord and peripheral nerve represents an unique example of unequal distribution of drugs. Most drugs, after they entered the body, can not distribute to the brain due to this barrier.

The most important route of excretion for most drugs is the kidney. There are two major mechanisms involved in renal excretion: glomerular filtration with variable tubular reabsorption and tubular secretion (Goth, 1981).

A compartmental model is a simplified mathematical description of a chemical's behavior in an animal, where the body is represented as a system of compartments. A compartment does not necessarily represent specific organs or

tissues, but rather represents tissue groups that are kinetically indistinguishable for a particular chemical (Barron *et al.*, 1990). Figure 1-6 illustrates some typical pharmacokinetic compartmental models.

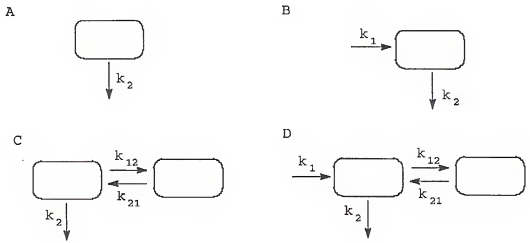

Figure 1-6. Schematic representation of rate constant based compartmental models: one compartment model with elimination (A); one compartment model with uptake and elimination (B); two compartment model with elimination (C); two compartment model with uptake and elimination (D). k_1 is the uptake rate constant, k_2 is the elimination rate constant, k_{21} and k_{12} are intercompartmental rate constants (Barron *et al.*, 1990).

The two primary assumptions of a compartmental model are instantaneous distribution and linear distribution (Gibaldi and Perrier, 1982). Instantaneous distribution means that once a chemical enters a compartment, it instantaneously distributes within the compartment. Linear distribution means that the concentration of chemical in every tissue associated

with a compartment is directly proportional to the amount of chemical in the compartment. While different tissues may have different concentrations of a chemical, a change in chemical concentration in one tissue will be accompanied by a proportional change in its concentration in all other tissues within the compartment. Non-linear kinetics (e.g. Michaelis-Menten kinetics in metabolism, membrane transport or protein binding) can be incorporated into a model if the non-linear process can be characterized experimentally (Bevill *et al.*, 1982).

Pharmacokinetic Modeling In Aquatic Animals

With continuing, rapid growth in the inventory of industrial chemicals, it has become clear that individual testing of compounds is impossible and that a predictive method is required. Fish and other aquatic organisms are exposed to chemicals in water and to chemicals complexed with food, particulates and dissolved organic material. Current interest in predicting the kinetics of chemical uptake and disposition has arisen because of the need to understand differences in species sensitivity and to permit extrapolation between different routes of exposure (Nichols *et al.*, 1990).

The most commonly used model is the compartmental model (Karara and Hayton, 1984; Barron *et al.*, 1988; Stehly and Hayton, 1989; James *et al.*, 1991). In practice, however, the limitations of curve fitting restrict such models to two or three compartments. More importantly, the use of

compartmental models for extrapolation is limited by the need to empirically fit a new set of parameters for each new compound, species and route of exposure.

One promising alternative to the compartmental model is the physiologically based kinetic model (Himmelstein and Lutz, 1979; Gerlowski and Jahn, 1983; Rowland, 1985). A physiologically based model defines an organism in terms of its anatomy, physiology and biochemistry. This leads to a better understanding of the disposition and toxicity of a chemical and provides a basis for extrapolation between species over a wide range of conditions. At present physiologically based toxicokinetic (PB-TK) models are being used in risk assessment (Clewell and Andersen, 1985; Andersen *et al.*, 1987) and have been successfully employed to extrapolate kinetic data between mammals (King *et al.*, 1983; Lutz *et al.*, 1984; Ramsey and Andersen, 1984). The PB-TK models has also been applied to fish (Zaharko *et al.*, 1972; Bungay *et al.*, 1976; Nichols *et al.*, 1990; Nichols *et al.*, 1991).

A simplified physiologically based pharmacokinetic (PB-PK) model for a chemical that is absorbed via the gill and metabolized irreversibly in the liver is shown in Figure 1-7.

Experiment Design

There are growing concerns about the effects of environmental pollutants on aquatic species and the potential for transfer of pollutants from seafood to human. Most of the

studies are concentrated on fish species. Shellfishes are also consumed as food, but there are fewer studies on these species. In this study, the aryl sulfotransferase and UDP-glucosyltransferase of the lobster will be characterized and the *in vitro* data will be fitted to the pharmacokinetic model.

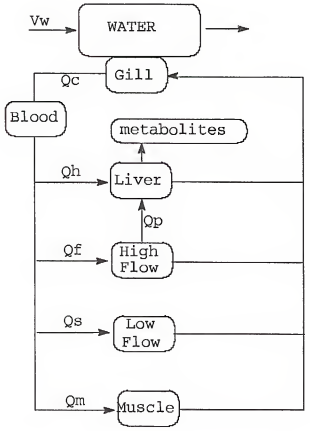

Figure 1-7. Schematic representation of a PB-PK model of a chemical that is absorbed by the gills and irreversibly metabolized in the liver. V_v: ventilation volume; Q_c: cardiac output; Q_h: hepatic arterial flow; Q_p: hepatic portal flow; Q_f: flow to kidney, spleen and G-I tract; Q_s: flow to fat and skin; Q_m: flow to muscle (From Barron *et al.*, 1990).

Aquatic Toxicology

Aquatic toxicology has been defined as the qualitative and quantitative study of adverse or toxic effects of chemicals and other anthropogenic material on aquatic organisms. This subject also includes the study of transport, distribution, transformation and ultimate fate of chemicals in the aquatic environment (Goksøyr and Förlin, 1992).

Metabolism of pollutants in aquatic organisms

Most of the aquatic species studied to date have some ability to metabolize the pollutants they take up, but to different extents. The most comprehensive work done on the phase 1 enzyme cytochrome P450 has been performed on the rainbow trout, the "guinea pig" of much fish research. From this species, workers in Buhler's laboratory have isolated five forms from ß-naphthoflavone (BNF)-treated fish, and five forms from untreated fish (Williams and Buhler, 1984; Miranda *et al.*, 1989). These isozymes belong either to CYP1A or CYP2B subfamilies (Goksøyr and Förlin, 1992). In mammals, the best characterized and well studied in the whole P450 superfamily is the CYP1A subfamily which consists of two genes, *CYP*1A1 and 1A2. Both of them can be induced by exogenous inducers such as BNF, polycyclic aromatic hydrocarbons (PAH) or 2,3,7,8-tetrachlorodibenzo-*p*-dioxin (TCDD) through the *Ah* receptor. However, only a single gene has been found in the fish species studied so far. In fish, the factors involved in P450 gene activation, including the *Ah* receptor, are not at all well

characterized. However, a number of studies have demonstrated the existence of P450 activities inducible by PAH-type inducers. 7-Ethoxyresorufin O-deethylase (EROD) and benzo[a]pyrene hydroxylase (AHH) activities appear to be the most sensitive catalytic probes for determining the induction response in fish. They also can be used as indicators of whether or not the animals have recently been exposed to this type of pollutant (Goksøyr and Förlin, 1992).

It has recently been established that CYP2B related genes are present and expressed in fish, but they are non-responsive to phenobarbital-type compounds. In contrast to fish, mammalian CYP2B subfamily can be induced by treatment with phenobarbital (Goksøyr and Förlin, 1992). All major phase 2 conjugation reactions reported in mammalian species are also present in aquatic species and have been reviewed (James, 1986; James, 1987; James, 1989b).

Bioconcentration and effects of pollutants on aquatic species

Bioconcentration is the phenomenon by which compounds are accumulated in organisms at a higher concentration than the surrounding environment. There is growing evidence that toxicants that are not extensively metabolized tend to move up the food chain. In a study with fathead minnows, the bioconcentration factors for 30 common organic chemicals were determined. Bioconcentration factors ranged from 2.7 for tris-(2,3-dibromopropyl)phosphate to 194,000 for Aroclor 1260. In another study, rainbow trout were exposed to radiolabelled

2,4,5-trichlorophenol and pentachlorophenol. In this case, bioconcentration factors of approximately 50-, 100-, 1000- and 10,000-fold for muscle, blood, liver and bile, respectively, were observed. In fact, these types of experiments may underestimate what would occur under natural conditions as the food items of feral fishes would most likely include organisms that had also accumulated contaminants (Malins and Ostrander, 1991).

Structural and functional alterations in cellular organelles can also provide a means of identifying and characterizing responses of cells to environmental contaminants. Furthermore, the identification of such changes increases the potential for understanding the mechanism(s) of a particular toxicant's effects as subcellular changes in organelles will usually precede an integrated cellular, organ or whole-animal response. An organelle receiving considerable attention among aquatic species is the lysosome. Studies with marine mollusks have demonstrated that, similar to mammals, lysosomes react to xenobiotics by increasing or deceasing lysosomal contents, the rate of membrane fusion events, or membrane permeability (Malins and Ostrander, 1991).

One study with seals fed either with fish from heavily polluted areas or relatively "clean" areas was conducted over a two-year period. The concentrations of individual polychlorinated biphenyl (PCB) congeners were measured in both the fish and seal blood. Significantly higher levels of PCBs

were found in both the fish from polluted areas and in the blood of seals fed these fish. Seals fed fish from polluted areas had significantly lower concentrations of plasma retinol, free thyroxin and triiodothyronine compared to seals fed fish from the "clean" areas. The PCB-induced reduction in plasma retinol concentrations was reversed when seals on polluted-area fish diet switched to clean-area fish. The authors speculate that the alterations in plasma retinol and thyroid hormone concentrations are critically involved in reproductive disorders and viral infections observed in seals (Malins and Ostrander, 1991). In another study with rainbow trout, the animals were exposed to either 2,3,7,8-tetrachlorodibenzo-*p*-dioxin or Aroclor 1254, and then challenged with infectious hematopoietic necrosis virus. Following viral challenge, virally induced histopathological lesions were more severe and occurred more frequently in toxicant-exposed fish as compared to controls (Malins and Ostrander, 1991).

Physiology Of American Lobster

There are four major families of decapod crustacea commonly referred to as "lobsters." The clawed lobsters (family Nephropidae) include the American lobster, *Homarus americanus* (Figure 1-8). The other three families do not carry claws. The Palinuridae, or spiny lobsters, so called because of the many spines on the carapace and basal segments

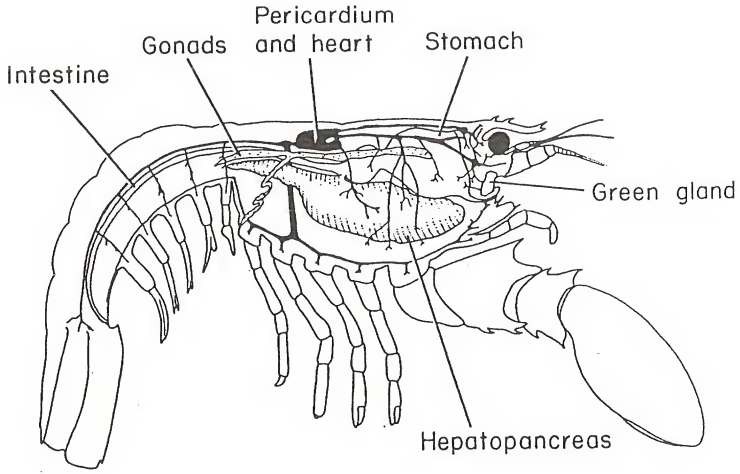

Figure 1-8. Schematic of the American lobster, *Homarus americanus*.

of the long second antennae, are also often referred to as rock lobsters and include the Florida spiny lobster, *Panulirus argus* (Cobb and Phillips, 1980).

The circulatory system of lobsters consists of (1) a muscular heart suspended in the pericardial sinus by three elastic ligaments, (2) thin-walled arteries that carry the blood (or hemolymph) away from the heart, eventually branching into much smaller vessels that open into tissue spaces, and (3) a series of irregular channels or sinuses developed from the primary body cavity, which conduct the blood back into the heart by way of the gills (Cobb and Phillips, 1980).

Blood enters the heart from the pericardial sinus through three pairs of valved slits (ostia). The heart is a single-chambered tube of striated tissue, which, in an adult lobster, makes up 0.1-0.15% of the total body weight. The heart beat rates of a 450 g *Homarus americanus* range from 50 to 136 beats per minute, with blood pressures that range from 9-22 mm Hg at systole to 0-5 mm Hg at diastole. The turnover time for the whole volume of blood was 1-8 minutes (Cobb and Phillips, 1980). The arterial system of *Panulirus interruptus* is outlined in Figure 1-9.

Total blood volume is variable but averages about 20% of the wet weight of the animal. There are two types of blood cells, hyaline and granular. Clotting of lobster blood is essentially different from the process that occurs in

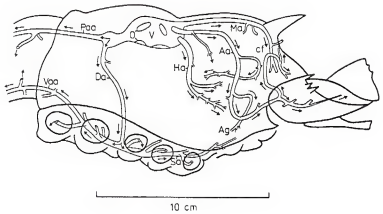

Figure 1-9. The arterial system of *Panulirus interruptus*. V, ventricle; O, ostial opening; Ma, median aorta; Aa, antennary artery; Ha, hepatic artery; Da, descending artery; Paa, posterior abdominal artery; Sa, sternal artery; Vaa, ventral abdominal artery; Ag, antennal gland; cf, region suggestive of cor-frontale (Cobb and Phillips, 1980).

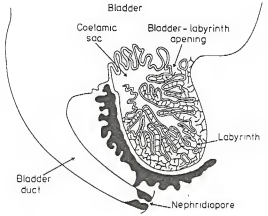

Figure 1-10. The antennal gland of *Panulirus* (Cobb and Phillips, 1980).

vertebrates. The hemolymph contains a dissolved fibrinogen, which is converted into fibrin in shed blood though the action of the thrombin-like catalyst termed coagulin. Coagulation begins with the disintegration of blood leukocytes, which release the coagulin. In the presence of Ca^{2+} ions, this factor accelerates the conversion of fibrinogen to fibrin, forming a homogeneous clot. Clotting can be prevented by the addition of magnesium sulfate or potassium oxalate to precipitate the Ca^{2+} ions. The blood pigment that assists oxygen carrying and storage capacity in the lobster is hemocyanin, a copper-containing pigment that appears light blue in the oxygenated condition (Cobb and Phillips, 1980).

Nitrogenous wastes, mainly ammonia, are excreted via the gills, the gut and to a lesser extent, the antennal or green glands. The paired antennal glands, which have functions similar to kidney, are found anterior to the ventral portion of the cardiac stomach and open through prominent papillae on the lower side of the basal segment of the first antenna. They are made up of two segments, a dorsal, thin-walled bladder and a ventral glandular section (Figure 1-10). The rate of urine output is about 0.5% of the body weight per day in American lobster. The primary urine is probably produced by ultrafiltration across an epithelial layer on the basement membrane that separates the lumen of the coelomosac from the blood supplied by the antennary artery. Ions such as Mg^{2+},

SO_4^{2-} and Cl^- are selectively excreted by the antennal glands (Cobb and Phillips, 1980).

The digestive tract of the lobster is relatively simple and is divided into three regions, the foregut, midgut and hindgut. The foregut region consists of the mouth, esophagus and a two-chambered stomach. The stomach is divided into an anterior cardiac portion and a posterior pyloric portion. The cardiac section of the foregut has a thick chitinous lining that is calcified in certain sections to form the gastric mill. The pyloric section of the stomach has a single dorsal caecum and a pair of ventrolateral ampullary filters. Here the food is sorted and strained and then directed back to the gastric mill, to the intestine, or to the hepatopancreas. The paired hepatopancreas (or digestive gland) which has functions similar to the liver of vertebrates is yellow-green in color and found on either side of the stomach and anterior portion of the midgut. There are openings from the hepatopancreas into the junction between the pyloric stomach and the midgut (Cobb and Phillips, 1980). Because lobsters are poikilotherm, elevated temperature accelerates the metabolic process and molt frequency.

Purpose Of The Study

As mentioned above, the marine environment is polluted with a number of lipophilic chemicals, some of which are carcinogens (Stegeman, 1981). In the United States, average fish and shellfish consumption was 11.8 pounds per person in

1970 and 15.5 pounds in 1990 (U.S. Department of Commerce, 1992). Marine crustacean species living in polluted environment are known to accumulate lipophilic organic chemicals, primarily into the hepatopancreas (James, 1989a). Studies have shown that hepatopancreatic microsomes from lobsters contained cytochrome P450 (James and Little, 1984) which can metabolize polycyclic hydrocarbons into phenolic and dihydrodiol metabolites similar to those formed by mammals (James, 1989c). Despite this, lobsters caught in polluted areas do not have tumors (Sindermann, 1979). There are few studies on the phase 2 metabolism of oxygenated metabolites formed from phase 1 metabolism in the lobster.

Preliminary *in vitro* studies showed that aryl sulfotransferase activity was found in the cytosolic fraction of the antennal gland and UDP-glucosyltransferase activity was found in both antennal gland and hepatopancreatic microsomes in American lobster, *Homarus americanus* (James *et al.*, 1987). No UDP-glucuronosyltransferase activity was detected. Studies are designed to characterize *in vitro* the aryl sulfotransferase and UDP-glucosyltransferase activities of the American lobster with respect to phenolic compounds. The second part of the study is to determine the half-life of some phenolic compounds *in vivo* and find the best kinetic model to describe the distribution and elimination of phenolic compounds in the American lobster.

Phenolic hydroxy groups are present in many drugs, pesticides and pollutants, or may be introduced by monooxygenation, or by hydrolysis of phenolic esters. Phenol which is very commonly used for this type of study (Capel *et al.*, 1972; Wheldrake *et al.*, 1978; Layiwola and Linnecar, 1981; Gorge *et al.*, 1987) is used as the first phenolic compound in this study. Lobsters caught in polluted areas might be exposed to or consume some food contaminated with benzo[a]pyrene which itself is biologically inactive and requires bioactivation to bind to DNA and exert its toxic, mutagenic and transforming effects. The potential carcinogen 3-hydroxybenzo[a]pyrene (3-OH BaP), which is a metabolite of benzo[a]pyrene, is used as second substrate in order to find out how the conjugating enzymes handle this chemical. In isolated hepatocytes from rat, the ratio of sulfate and glucuronide conjugates formed (Orrenius *et al.*, 1978) and the rate of glucuronidation (Fry and Paterson, 1985) are related to the lipophilicity of the chemical. For this objective, ß-naphthol is used as compound with intermediate lipophilicity to find out what effect changing the lipophilicity will have on the conjugating enzymes. The pK_as of the three phenolic compounds used are very similar, but they have increasing lipophilicity. The structure and octanol/water partition coefficient (expressed as log P values) of compounds used are shown in Figure 1-11.

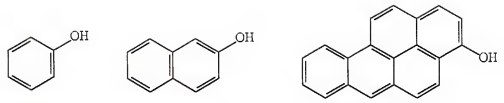

Phenol

log P 1.46

β-Naphthol

log P 2.84

3-Hydroxy-BaP

log P_{calcd} 6.34

Figure 1-11. The structures and log P values of compounds used (Log P values were from Leo *et al.*, 1971).

Using a pharmacokinetic model to describe the distribution and elimination of toxic chemicals in animals can help us to predict which organ is more vulnerable and where the chemicals are stored. A better understanding of the role that sulfate and glucoside conjugating enzymes play in the low concentration range may help in predicting the expected metabolites of phenolic compounds formed in crustacea.

CHAPTER 2
MATERIALS AND METHODS

Materials

Chemicals

[^{14}C]-labelled phenol with specific activities of 5.0 to 9.6 mCi/mmol and 99% radiochemical purity, [^{14}C]-labelled ß-naphthol with a specific activity of 9.8 mCi/mmol and 99% radiochemical purity, deuterium oxide (D_2O), adenosine 3'-phosphate 5'-phosphosulfate lithium salt (PAPS, 75%-87% purity), ß-mercaptoethanol, sucrose, sodium chloride, N-ethylmaleimide, triethanolamine (TEA), ethylenediamine tetraacetic acid (EDTA) disodium salt, adenosine 3',5'-diphosphate (PAP), adenosine 3'-monophosphate (3'-AMP), PAP-agarose gel, silica gel (70-230 mesh), UDP-glucose, UDP-glucuronic acid, Lubrol PX, alkaline phosphatase (EC 3.1.3.1) type III from bacterium (*Escherichia coli*), arylsulfatase (EC 3.1.6.1) type V from limpets (*Patella vulgata*), arylsulfatase (EC 3.1.6.1) type VI from bacterium (*Aerobacter aerogenes*), ß-glucosidase (EC 3.2.1.21) type II from almonds, *p*-nitrophenol, *p*-nitrophenyl conjugates, ß-naphthol, ß-naphthyl glucoside, phenyl phosphate, α- and ß- linked conjugates of phenol with glucose, glucuronic acid, galactose and N-acetylglucosamine were purchased from Sigma Chemical company. Chlorosulfonic

acid, N,N-diethylaniline and ß-naphthyl sulfate potassium salt with 93% purity were received from Aldrich Chemical company. Crystallized, ultrapure Tris(hydroxymethyl)aminomethane (Tris) free base was obtained from Boehringer Mannhein Biochemicals. Ultrafree-MC 10,000 NMWL filters, 0.45 μm filters, Sep-Pak® alumina N. and C18 cartridges were purchased from Millipore® Waters Associate. XAD-2 minicolumns were obtained from either Isolab Inc. or Alltech Associate Inc. DEAE-cellulose (Whatman DE-52) was from Whatman Labsales. Sodium dodecyl sulfate (SDS) and chemicals used in polyacrylamide gel electrophoresis were obtained from Bio-Rad Laboratories. Centrisart® centrifuge tubes with 10,000 molecular weight cutoff membrane were purchased from Vanguard International Inc.. All HPLC grade solvents and phenol were purchased from Fisher Scientific company.

3-Hydroxybenzo[a]pyrene (3-OH BaP) and benzo[a]pyrene 3-sulfate (BaP 3-sulfate) were received from the NCI Chemical Carcinogen Reference Standard Repository, a function of the Division of Cancer Etiology, NCI, NIH, Bethesda, Maryland. [^{3}H]3-OH BaP with specific activity of 417.1 mCi/mmol and nominal 98% radiochemical purity was purchased from Chemsyn Science Laboratories (Lenexa, KS). The [^{3}H]3-OH BaP readily decomposed to the 3,6-quinone and was purified by reverse phase HPLC with 50% methanol as the mobile phase, or by solvent extraction. The impure 3-OH BaP was dissolved in 10 ml 1 N NaOH, then extracted with 2×10 ml hexanes. The aqueous

phase was acidified with 5 N HCl to pH 4, then extracted with 2×10 ml hexanes. The purity of the [^{3}H]3-OH BaP as used in assays was greater than 90%, as determined by reverse phase HPLC coupled with radiochemical detection.

Phenyl sulfate sodium salt and ß-naphthyl sulfate sodium salt were synthesized by the method of Burkhardt (1926). An aliquot of 10 g N,N-diethylaniline was dissolved in 10 ml chloroform and this solution was cooled to -10°C. Then an aliquot of 2.5 ml, 37.6 mmol, chlorosulfonic acid was added drop-wise to the solution within 15 minutes while the temperature was kept below 10°C to form the N,N-diethylaniline sulfur trioxide complex (Gilbert, 1965). Phenol solution, 2.2 g phenol in 5 ml chloroform, or ß-naphthol solution, 5.4 g ß-naphthol in 5 ml chloroform, was poured into the solution of the complex all at once. The mixture was stirred for one hour for phenol, two hours for ß-naphthol. The reaction was terminated by adding sodium hydroxide solution, 2.2 g sodium hydroxide in 15 ml water. Then the mixture was adjusted to pH 7 with more 1 N sodium hydroxide solution and the aqueous phase was extracted with chloroform to remove traces of N,N-diethylaniline. The aqueous phase was dried under vacuum and the crude product was recrystallized with 95% ethanol. The product, phenyl sulfate sodium salt, was checked by IR, NMR, HPLC, UV and enzymatic hydrolysis. Standard phenyl sulfate potassium salt was purchased from American Tokyo Kasei Chemical company and purified by extraction with a solution of

acetone/toluene, 1:1, before chemical analyses. ß-Naphthyl sulfate was checked by NMR, HPLC and enzymatic hydrolysis.

Instruments

The following instruments were used in this study. Two HPLC systems were used, one isocratic with an Isco HPLC pump model 2300 coupled with a UA-5 UV detector and the other a gradient HPLC system. The gradient HPLC had a Beckman HPLC system controller model 421A , two HPLC pumps model 110B, an analytical UV detector model 153, a Shimadzu fluorescence detector and a Radiomatic flo-one *beta* radioactive flow detector. Spectrophotometers used were Perkin-Elmer fluorescence spectrometer model LS-3B, 1420 ratio recording infrared spectrophotometer, Varian EM-390 90 MHz NMR spectrometer and Shimadzu UV-VIS spectrophotometer model UV-265. The tissue oxidizer used was a Parkard Tri-Carb® sample oxidizer model B 306. Liquid scintillation systems used were Parkard Tri-Carb® liquid scintillation system model 460CD and Beckman liquid scintillation system model LS 5000 TD. Centrifuges used were Beckman ultracentrifuge model L8-80M and Du Pont Sorvall® centrifuge model RC2-B.

Methodologies

In Vitro Studies

Animals and preparation of subcellular fractions

Lobsters were anesthetized by placing on ice before dissection. The lobsters used were purchased from restaurant

suppliers and had body weights of 450 - 650 g. The lobsters were held in 14 ± 2°C fresh flowing sand-filtered seawater for at least one week before use in studies. Lobsters were molt-staged by examination of sections of pleopod (Aiken, 1973). Although animals from several molt stages were studied, comparisons were made only with intermolt animals. The antennal glands from American lobsters were blotted before weighing, then homogenized with 4 weight volumes of TES buffer (0.05 M Tris/HCl, pH 7.2, 0.01 M EDTA, 0.25 M sucrose). The homogenates were centrifuged at 13,300*g* for 20 minutes at 4°C. The supernatants were centrifuged again at 150,000*g* for 45 minutes at 4°C. The ensuing supernatants (cytosolic fractions) were used as the source of aryl sulfotransferase and the 150,000*g* pellets (microsomal fractions) were pooled, re-suspended in 3 volumes of TES buffer and used in assays of UDP-glucosyltransferase activity. The same protocol was used to prepare microsomal and cytosolic fractions from the hepatopancreas. The protein content of each fraction was determined by the method of Lowry *et al.* (1951) using bovine serum albumin as a standard.

HPLC analysis

The purity of each substrate and the identity of each reaction product was checked by HPLC with UV and radiochemical detection. There were two HPLC columns used throughout this study. Column A: the stationary phase was an Altex 5×0.45 cm ultrasphere ODS guard column coupled to a 25×0.45 cm

analytical ultrasphere ODS column. Column B: the stationary phase was a Whatman ODS cartridge column, 15×0.45 cm. For phenol, the mobile phase used for system A was 10 mM potassium phosphate, pH 2.75/acetonitrile, 4:1 (V/V) and 19:1 (V/V) for system B. For ß-naphthol, system A was used and the mobile phases were 10 mM potassium phosphate, pH 2.74/acetonitrile 3:2, 7:3 and 4:1 (V/V). For 3-OH BaP, system A was used and 86.5% methanol/water (V/V) was used as mobile phase. Retention times were 2.9 minutes for BaP 3-sulfate, 5 minutes for BaP 3-glucoside and 12.8 minutes for 3-OH BaP.

Aryl sulfotransferase assays

Assay tubes contained 0.1 M sodium phosphate buffer, pH 7.2; 70 μl cytosolic fraction containing 0.1-0.3 mg protein; 5-400 μM PAPS; 4-100 μM [^{14}C]-phenol, 30-300 μM [^{14}C]-ß-naphthol or 10-60 μM [^{3}H]-3-OH BaP; and deionized water to a final volume of 250 μl. For 3-OH BaP, the buffer solution used was 0.5 M sodium phosphate buffer, pH 7.0. The reactions were started by adding either the PAPS or the phenolic substrate and tubes were incubated at 35°C (Elmamlouk and Gessner, 1978) for 30 minutes. For phenol and ß-naphthol, the reactions were terminated by adding 3 ml water saturated ethyl acetate. The blanks had 3 ml ethyl acetate added immediately after the co-substrate was added. All samples were extracted with 2×3 ml ethyl acetate, vortexed for 1 minute and centrifuged at 1,500 rpm for 10 minutes. The efficiency of extraction was tested by dissolving substrate and metabolite

standards in the buffer solution, and analyzing the organic and aqueous phases by UV spectrophotometry or by reverse phase HPLC. For each sample, an aliquot of 125 μl of the aqueous phase was directly assayed for [^{14}C] by liquid scintillation spectrometry. For 3-OH BaP, a mixture of hexanes was used instead of ethyl acetate and the aqueous phase was assayed for [^{3}H] by liquid scintillation spectrometry.

UDP-glucosyltransferase assays

For measurement of UDP-glucosyltransferase activity with phenol or ß-naphthol, assay tubes contained 0.1 M glycine-sodium hydroxide buffer, pH 10.4; 0.2-2.6 mM UDP-glucose or UDP-glucuronic acid; 0.25-5 mM [^{14}C]-phenol or [^{14}C]-50-500 μM ß-naphthol; 0.1 mg microsomal protein; and deionized water to a final volume of 200 μl. TES buffer solution with 0.1% lubrol (W/V) was used to dilute the microsomes to the desired concentration. For the pH profile, 0.5 M sodium phosphate buffers ranging from pH 5.5 to 8.5 and 0.5 M glycine-sodium hydroxide buffers ranging from pH 8.5 to 12.7 were used in the assays. The actual pH was measured after all reactants were added. The reaction was started by adding the phenolic substrate or the UDP glucose, then the tubes were incubated at 35°C for 20 minutes. An aliquot of 3 ml toluene was added to stop the reaction. All samples were extracted with 2×3 ml toluene, vortexed for 1 minute and centrifuged at 1,500 rpm for 10 minutes. An aliquot of 100 μl of the aqueous phase was directly assayed for [^{14}C] by liquid scintillation

spectrometry. The extraction efficiencies were verified with standards. For 3-OH BaP, unlabelled compound was used; the concentration range tested was 4-24 μM; tubes contained 1.75 mg hepatopancreas microsomes or 0.1 mg antennal gland microsomes; the final volume was 500 μl; and 2.5 ml of 0.1 N sodium hydroxide were added to terminate the reaction. Glycine-sodium hydroxide, 0.1 M, pH 9.5, was used as the buffer in assays of hepatopancreas and antennal gland UDP-glucosyltransferase activities with 3-OH BaP. The activity of UDP-glucosyltransferase was measured by following the disappearance of the parent compound by fluorescence spectrophotometry (excitation at 455 nm, emission at 520 nm).

Purification of antennal gland aryl sulfotransferase

The antennal gland cytosolic fractions prepared as described were dialyzed against 10 mM TEA, pH 7.4, containing 10% glycerol and 5 mM ß-mercaptoethanol. All purification procedures were performed at 4°C. The dialyzed cytosolic fractions were applied to a DEAE-cellulose column (1.6×30 cm) which had previously been equilibrated in dialysis buffer and washed with the same buffer overnight. The aryl sulfotransferases were eluted from the anion-exchange column with a 580 ml linear NaCl gradient (0-250 mM) in dialysis buffer. Fractions of 6 ml were collected and those fractions containing aryl sulfotransferase activity were pooled and loaded onto a PAP-agarose affinity column (1×8 cm) equilibrated in 100 mM TEA buffer, pH 7.4. The affinity

column was sequentially washed with 20 ml of TEA buffer, 20 ml of TEA buffer containing 50 mM NaCl and 20 ml TEA buffer containing 50 mM NaCl and 500 μM 3'-AMP. Aryl sulfotransferase activity was then eluted with a 20 ml linear gradient (0-1,000 μM) of PAP in TEA buffer containing 50 mM NaCl. Fractions of 2 ml were collected and then individually concentrated to approximately 0.1 ml with a 10,000 NMWL filter. All samples were checked by electrophoresis.

SDS-polyacrylamide gel electrophoresis (SDS-PAGE)

Polyacrylamide gel electrophoresis was performed in the presence of SDS in a Bio-Rad Mini-Protein® II unit as previously outlined by Laemmli (1970). Samples were pretreated with sample buffer to final concentration of 20%, and then heated to 95°C for 4 minutes. Following electrophoresis the gels were stained with either Coomassie blue or silver stain. Molecular weights of the purified samples were compared with Bio-Rad low molecular weight standards.

Statistical analysis

Lotus 1-2-3® software was used to perform the linear regression analyses. Excel® software was used to analyze data for statistical significance by Student's *t* test.

Calculation of K_m and V_{max} from the Michaelis-Menten equation

The Michaelis-Menten equation (2-1) may be inverted and factored as follows:

$$[V] = \frac{V_{max} \times [S]}{K_m + [S]} \qquad (2\text{-}1)$$

Invert:

$$\frac{1}{[V]} = \frac{K_m + [S]}{V_{max} \times [S]} \qquad (2\text{-}2)$$

Factor:

$$\frac{1}{[V]} = \frac{K_m}{V_{max}} \times \frac{1}{[S]} + \frac{[S]}{V_{max} \times [S]} \qquad (2\text{-}3)$$

$$\frac{1}{[V]} = \frac{K_m}{V_{max}} \times \frac{1}{[S]} + \frac{1}{V_{max}} \qquad (2\text{-}4)$$

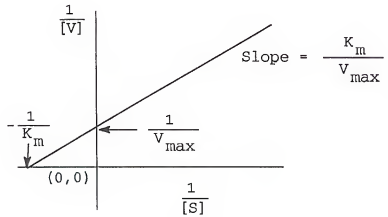

Figure 2-1. Lineweaver-Burk plot of 1/[V] versus 1/[S] used for graphic evaluation of K_m and V_{max}.

This is the equation (2-4) for a straight line. Using linear regression analysis for the Lineweaver-Burk plot of 1/[V] versus 1/[S] (Figure 2-1), V_{max} can be calculated by inverting the y intercept and K_m can be derived from the slope.

In Vivo Studies

Lobsters

Experiments were conducted at Whitney Laboratory, Florida. The treated lobsters were held singly in tanks with rapidly flowing seawater at 14 ± 2°C, except that in experiments to determine excretion into tank water, the lobsters were held for 30 minutes after injection in a small tank containing 2 liters fresh seawater, and thereafter sacrificed or transferred to a flow-through tank for the duration of the experiment. Some animals were externally cannulated from their nephropores to collect urine (Holliday, 1977, Snyder and Chang, 1991). All animals were intermolt and weighed 500 ± 60 g.

Treatment

Animals were injected intrapericardially with [^{14}C]-labelled phenol or ß-naphthol dose solution in saline (0.9% NaCl solution). Serial hemolymph samples (1-2 ml) were taken from the appendage joints. Duplicated aliquots of each hemolymph sample (0.1 ml) were pipetted immediately into vials containing scintillation cocktail, and the remainder of each

sample was placed in a tube containing 0.1 g N-ethylmaleimide to inhibit clotting. At the time of sacrifice, animals were placed in ice and terminal hemolymph samples (5-10 ml) removed from the pericardial sinus. Terminal urine samples were collected from urinary papillae, and other organs were dissected and stored at -20°C before chemical analysis. Triplicate 2 ml samples of the 30 minutes tank water were directly assayed for [^{14}C].

Tissue distribution

Samples of hemolymph and urine (0.1 ml) were directly assayed for [^{14}C] by liquid scintillation spectrometry. Duplicate organ samples, 0.1 g, were completely oxidized by the tissue oxidizer to [^{14}C]-CO_2 prior to [^{14}C]-spectrometry.

Chemical analyses

The hemolymph samples, 0.5 - 1 ml, were deproteinized by thoroughly mixing with 2×3 ml acetonitrile. To the pooled acetonitrile extracts, 10 ml of 0.1 M ammonium chloride/ammonia buffer, pH 10 was added, and the acetonitrile was removed by evaporation under nitrogen. The solution was made up to 15 ml with the 0.1 M ammonium chloride/ammonia buffer, pH 10, and applied to an XAD-2 minicolumn. The XAD-2 minicolumns were sequentially washed with 5 ml deionized water, 5 ml methanol, 10 ml deionized water and 10 ml 0.1 M ammonium chloride/ammonia buffer, pH 10, before use. For phenol samples, the column was washed with 15 ml of the same

buffer, then 1 ml acetone and 20 ml mixture of chloroform/methanol, 3:1. The last step was to wash the column with 10 ml of a mixture of chloroform/methanol, 3:1. For ß-naphthol samples, an aliquot of a 15 ml mixture of acetone/0.1 M ammonia buffer, pH 10, 3:7, was used to wash the column instead of 1 ml acetone. An aliquot of 1 ml of each eluent was directly assayed for [^{14}C] by liquid scintillation spectrometry. The elution pattern of the unlabelled conjugates was determined by UV scans of each fraction.

A sample of the tank water which held the lobster for the first 30 minutes, 20 ml, was extracted with 2×10 ml water saturated ethyl acetate. The combined ethyl acetate extracts were dried under nitrogen, then the residue was dissolved in the mobile phase prior to reverse phase HPLC analysis.

Metabolites hydrolyses

The metabolite composition of urine, urine extract, or hemolymph extract was investigated by HPLC analysis and by determining the stability of the metabolites to several hydrolytic enzymes and to dilute acid.

Samples of urine or urine extracts were adjusted to the appropriate pH with one-tenth volume of 1 M sodium acetate buffer, pH 5, 0.1 M Tris/HCl, pH 7, or 1 M ammonium chloride/ammonia buffer, pH 10. The urine solutions were incubated with 0.78 units of ß-glucosidase type II from almonds (pH 5), or 0.3 units of alkaline phosphatase type III from bacterium (*Escherichia coli*) (pH 10), or 1.2 units of

arylsulfatase type V from Limpets (*Patella vulgata*) (pH 5), or 0.14 units of arylsulfatase type VI from bacterium (*Aerobacter aerogenes*) (pH 7) at 37°C overnight then reanalyzed by HPLC. Urine samples were also incubated with 1 N or 2 N HCl at 37°C overnight and reanalyzed by HPLC.

The activity of each enzyme under the above incubation conditions was monitored by adding the appropriate *p*-nitrophenyl conjugates to separate urine samples, hemolymph extracts, or buffer, and monitoring enzyme-catalyzed liberation of *p*-nitrophenol. After incubation, an aliquot of 2.5 ml 0.1 N NaOH was added. The amount of *p*-nitrophenol formed was determined by comparison of the absorbance at 420 nm with that of similarly prepared samples of *p*-nitrophenol at known concentrations.

Enzymatic synthesis of [^{14}C]-labelled phenyl sulfate

Fresh female rat liver was homogenized in a Potter-Elvehjem homogenizer with 3 volumes of homogenization buffer (0.05 M sodium phosphate buffer, pH 7.6, 1.15% potassium chloride). The homogenate was centrifuged at 13,300*g* for 10 minutes and then 150,000*g* for 45 minutes at 4°C. The 150,000*g* supernatant was used as the enzyme source and 10,000 NMWL PLGC filters were used to filter the enzyme to remove low molecular weight proteins. Assay tubes contained [^{14}C]-labelled phenol with specific activity 5 mCi/mmol, 0.02 μmol, and 50 μl PAPS, 0.2 mg in 300 μl 0.1 M sodium phosphate buffer, pH 6.5. The reaction was initiated by adding 50 μl enzyme, mixing well and

incubating at 35°C for 5, 10, 20 and 60 minutes. After incubation, an aliquot of 50 µl acetonitrile was added to terminate the reaction. The products were then centrifuged at 1,500 rpm for 10 minutes to precipitate the proteins. The supernatants were filtered with 0.45 µm filters before analysis by reverse phase HPLC system coupled with a radioactivity detector to check the retention time of the products.

Isolation and identification of major phenol-dosed lobster urinary metabolite

The urine samples were pooled in a 50 ml round bottom flask and the rotatory evaporator was used to evaporate the samples to dryness. An aliquot of 3 ml acetone was used to extract the urine residue, with sonication if necessary. The acetone extraction was repeated twice. A Sep-Pak Alumina N. cartridge was prepared by washing with 5 ml methanol then 6 ml acetone. The acetone extract was passed through the cartridge and the eluent was collected into test tube # 1. The graduated cylinder that held the extract was rinsed with 6 ml acetone and this 6 ml acetone passed through the cartridge into test tube # 2. The cartridge was eluted with 2×3 ml methanol and the eluents were saved in test tubes # 3 and # 4. The cartridge was next eluted with 2×6 ml deionized water and the eluents placed in test tubes # 5 and # 6. Then the cartridge was eluted with 6 ml and 3 ml 1 M acetic acid and the eluents were collected in test tubes # 7 and # 8,

respectively. Samples, 0.1 ml, were taken from each eluent fraction and put in a 7 ml scintillation vial with 5 ml scintillation cocktail for scintillation spectrometry.

The eluents with radioactivity were pooled and evaporated to dryness under vacuum. The residues were extracted with 3×3 ml acetone, and the solutions were placed in a cylinder. An equal amount of toluene was added to the acetone extract to make an acetone/toluene solution, 1:1. Acetone/toluene solution,1:1, was used as the mobile phase to set up a silica gel column. The urine extract was loaded onto the column and more acetone/toluene solution, 1:1, was used to rinse out the graduated cylinder and make the final volume of acetone/toluene, 1:1, 100 ml. The column was eluted with the rinsed acetone/toluene solution, 1:1, and the eluent was collected into a 200 ml flask. The column was then eluted with 100 ml acetone/toluene solution, 3:2, and fractions of 10 ml were collected into test tubes # 1 to # 10. The column was washed with 100 to 200 ml of acetone/toluene solution, 7:3, and fractions of 10 ml were collected into 100×16 mm test tubes. The last step was to wash the column with acetone, 100 ml, and the eluent was collected into a 200 ml flask. An aliquot of 1 ml sample was taken from the well mixed acetone/toluene, 1:1, and acetone eluents and placed into a 20 ml vials with 10 ml cocktail for analysis of [^{14}C]. For the individual fractions, 0.1 ml aliquots were analyzed for [^{14}C].

Preparation of FAB-MS samples

The purified phenol conjugate, about 450 μg phenol equivalent, and 50 mg partially decomposed phenyl sulfate potassium salt were separately dissolved in 10 ml deionized water and placed in 125 ml separatory funnels. An aliquot of 1 ml 40% tetrabutylammonium hydroxide solution was added to the samples and the samples were shaken vigorously for 30 seconds. Chloroform, 3×5 ml, was used to extract the samples and the chloroform extract was dried under nitrogen. The matrix for the FAB-MS was glycerol and the positive ion mode was used.

Hemolymph protein binding

Lobsters were injected with varying doses of phenol in the range of 0.05 to 2.0 mg/kg, and samples of hemolymph, 2.5 ml, were taken at 1, 2 and 30 minutes after the dose. In other experiments, lobsters were dosed with 0.25 mg/kg ß-naphthol and samples of hemolymph were taken at 1 minute, 24 hours and 120 hours after injection. Duplicate 0.1-ml portions of each sample were placed immediately in vials containing scintillation cocktail. The remaining hemolymph, 2 ml, was placed immediately in the lower chamber of a prechilled Centrisart® tube containing a 10,000 molecular weight cutoff membrane attached to an upper tube. The Centrisart® tubes were centrifuged immediately at 2,500 rpm for 10 minutes in a refrigerated (4°C) centrifuge. Under these conditions , 3 to 8% of the total sample volume was

recovered as ultrafiltrate. Samples of the ultrafiltrate collected in the upper tube were analyzed for [^{14}C] by scintillation spectrometry.

Pharmacokinetic analysis

A two-compartment pharmacokinetic model (Simusolv®, Dow Chemical Company), was used to analyze the data collected on phenol concentrations in hemolymph at various time points after the dose. The half-life of elimination of phenyl sulfate from hemolymph was determined by linear regression analysis of the log of phenyl sulfate concentration in hemolymph versus time from 2 to 24 hours after the dose for males, and from 4 to 24 hours after the dose for females. For ß-naphthol, Rstrip® and PCNONLIN® softwares were used to fit the data and estimate parameters which were used in the equation to describe the plasma concentration of parent compound.

Pharmacokinetic models used in pharmacokinetic analyses

For both phenol and ß-naphthol, a typical two-compartment model, Model A, with i.v. administration was used to estimate parameters which were used in describing the plasma concentration of parent compounds. Pharmacokinetic model with Michaelis-Menten elimination kinetics, Model B, was also used for ß-naphthol to describe the plasma concentrations of metabolites formed *in vivo*. Both models are shown in Figure 2-2.

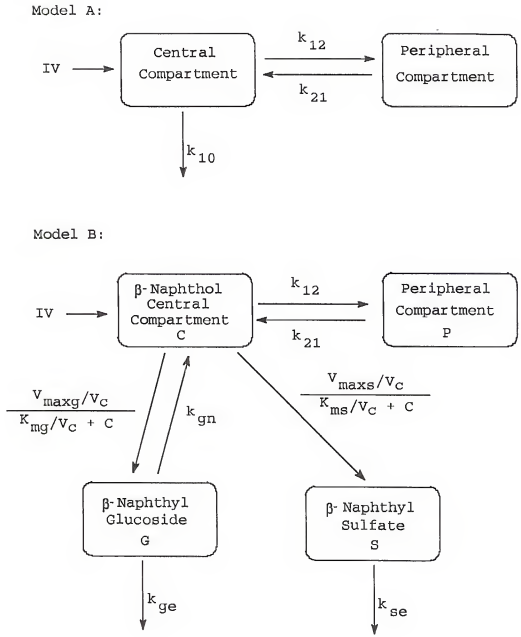

Figure 2-2. Pharmacokinetic models used. Model A is a typical two-compartment pharmacokinetic model. Model B is a model with Michaelis-Menten elimination kinetics.

The units of K_m and V_{max} were converted from μM and pmol/min/mg protein to ng/ml and ng/min/ml (Dedrick et *al.*, 1972; Dedrick and Bischoff, 1980) by the following equations. For K_m:

$$\frac{K_m \times M.W. \times V \times P \times O.W. \div P.U.}{V_c} \qquad (2\text{-}5)$$

Where: K_m is expressed as μmol/l, M.W. is molecular weight and expressed as μg/μmol, V is final volume in each assay and expressed as ml, P is the amount of cytosolic or microsomal protein in tissue and expressed as mg/g tissue, O.W. is organ weight and expressed as g tissue/kg of body weight, P.U. is the amount of cytosolic or microsomal protein used in each assay and expressed as mg, V_c is the volume of central compartment and expressed as $ml \times kg^{-1}$.

For V_{max}:

$$\frac{V_{max} \times P \times O.W. \times M.W. \div 1000}{V_c} \qquad (2\text{-}6)$$

Where: V_{max} is expressed as pmol/min/mg protein, P is the amount of cytosolic or microsomal protein in tissue and expressed as mg/g tissue, O.W. is organ weight and expressed as g tissue/kg of body weight, M.W. is molecular weight and expressed as μg/μmol, V_c is the volume of central compartment and expressed as $ml \times kg^{-1}$.

The following differential equations were used to define the compartments in Model B:

Central compartment, C, was defined in Equation 2-7:

$$dC(C)/dt = k_{21}\times C(P) + k_{gn}\times C(G) - k_{12}\times C(C) - \{(V_{maxg}/V_c)/[(K_{mg}/V_c)+C(C)]\}\times C(C) - \{(V_{maxg}/V_c)/[(K_{mg}/V_c)+C(C)]\}\times C(C) \quad (2\text{-}7)$$

Compartment for ß-naphthyl glucoside, G, was defined in Equation 2-8:

$$dC(G)/dt = \{(V_{maxg}/V_c)/[(K_{mg}/V_c)+C(C)]\}\times C(C) - k_{ge}\times C(G) - k_{gn}\times C(G) \quad (2\text{-}8)$$

Compartment for ß-naphthyl sulfate, S, was defined in Equation 2-9:

$$dC(S)/dt = \{(V_{maxs}/V_c)/[(K_{ms}/V_c)+C(C)]\}\times C(C) - k_{se}\times C(S) \quad (2\text{-}9)$$

Peripheral compartment, P, was defined in Equation 2-10:

$$dC(P)/dt = k_{12}\times C(C) - k_{21}\times C(P) \quad (2\text{-}10)$$

Calculation of parameters estimated from two-compartment model

Equation 2-11 was used to describe the plasma concentration of parent compound (Cp) over time (t) after i.v. injection for a two-compartment model.

$$C_p = A \times e^{-\alpha t} + B \times e^{-\beta t} \quad (2\text{-}11)$$

A, B, α and ß can be obtained from either semilogarithmic plot of concentration versus time or computer software. The half-lives for the distribution (α) and elimination (ß) phases were calculated from equation 2-12.

$$t_{1/2\alpha \text{ or } \beta} = \frac{0.693}{\alpha \text{ or } \beta} \qquad (2\text{-}12)$$

The rate constants describing the movement of parent compound between compartments (k_{12} and k_{21}) and elimination from the body (k_{10}) were obtained from the following equations:

$$\alpha + \beta = k_{12} + k_{21} + k_{10} \qquad (2\text{-}13)$$

$$\alpha \times \beta = k_{21} \times k_{10} \qquad (2\text{-}14)$$

$$k_{21} = \frac{(A\alpha + B\beta)}{A + B} \qquad (2\text{-}15)$$

$$k_{10} = \frac{\alpha \times \beta}{k_{21}} \qquad (2\text{-}16)$$

$$k_{12} = \alpha + \beta - k_{21} - k_{10} \qquad (2\text{-}17)$$

Area under the concentration-time curve (AUC), volume of distribution (V_d), volume of central compartment (V_1), volume of peripheral compartment (V_2), whole body clearance (Cl_b) and intercompartmental clearance (Cl_t) were calculated from the following equations:

$$AUC = \frac{A}{\alpha} + \frac{B}{\beta} \qquad (2\text{-}18)$$

$$V_d = \frac{Dose}{\beta \times AUC} \qquad (2\text{-}19)$$

$$V_1 = \frac{Dose}{A + B} \qquad (2\text{-}20)$$

$$V_2 = \frac{k_{12}}{k_{21}} \times V_1 \qquad (2\text{-}21)$$

$$Cl_b = \frac{Dose}{AUC} \qquad (2\text{-}22)$$

$$Cl_t = V_1 \times k_{21} \quad or \quad V_2 \times k_{12} \qquad (2\text{-}23)$$

The half-lives are expressed in time, volumes in $ml \times kg^{-1}$, AUC in $mg \times min \times ml^{-1}$ and clearances in $ml \times min^{-1} \times kg^{-1}$.

CHAPTER 3
RESULTS AND DISCUSSION

When studying the fate of xenobiotics in species such as the American lobster, whose biochemical make-up is poorly studied, it is desirable to conduct both *in vivo* and *in vitro* studies to provide information on the pathways of biotransformation of common functional groups.

In Vitro Studies

Results

Aryl sulfotransferase

The efficiencies of solvent extraction were greater than 95% for removing unreacted substrates. Less than 2% of the sulfate conjugates were extracted. As found previously, only the cytosolic fraction of antennal gland had sulfotransferase activity. The optimum pH for the assay of sulfotransferase activity varied with different acceptor molecules as shown in Figure 3-1. Phenol sulfotransferase had no clear optimal pH in the range studied. With ß-naphthol the pH optimum for males was 7.5 and 6.7 for females, and with 3-OH BaP the pH optimum was 6.3 for both males and females.

The apparent K_m and V_{max} values of aryl sulfotransferase activity from American lobster antennal gland for different phenolic substrates are tabulated in Table 3-1. The apparent

K_m and V_{max} values for the co-substrate PAPS with different phenolic substrates are tabulated in Table 3-2. The data shown in Tables 3-1 and 3-2 are for intermolt lobsters only. The antennal gland aryl sulfotransferase had the highest affinity for phenol, but V_{max} was lowest. K_m and V_{max} values for ß-naphthol and 3-OH BaP were similar (Table 3-1). For phenol and 3-OH BaP, the females had higher V_{max} than males ($P < 0.05$). No such difference was observed for ß-naphthol (Table 3-1). For all phenolic substrates, K_m values were more variable in individual females than males, and this was especially true for ß-naphthol. The apparent K_m for PAPS was higher in females than males with phenol or ß-naphthol as substrate, and V_{max} with ß-naphthol was also significantly higher in females under the conditions used (Table 3-2). A typical Lineweaver-Burk plot for the determination of the apparent PAPS K_m of aryl sulfotransferase in a female lobster with 52 μM phenol as substrate is shown in Figure 3-2. No sex difference was found with 3-OH BaP as substrate.

In measuring the K_m for PAPS with ß-naphthol, a total of eight female lobsters were studied, with different gonad/body weight ratios, and in different molt stages. The apparent K_m for PAPS ranged from 7.1 to 205 μM. In the small number studied, there was no correlation of apparent K_m for PAPS with gonadal maturity. Three lobsters with gonadal weights accounting for 0.9, 1.5 and 3% of body weight had apparent K_ms for PAPS of 85 μM, 20 μM and 205 μM respectively. The gonads

Table 3-1. The apparent K_m and V_{max} values of sulfotransferase from both male and female American lobster antennal glands for different substrates.

Substrate	Sex	K_m	V_{max}
Phenol	♂	11.6 ± 0.6*	5.8 ± 1.5*
	♀	22.4 ± 8.5*	20.1 ± 11.4*
ß-Naphthol	♂	69.5 ± 9.9	108 ± 72.9
	♀	112 ± 36.4	360 ± 256
3-OH BaP	♂	41.8 ± 5.8	56.9 ± 17.7*
	♀	35.6 ± 13.1	94.9 ± 12.3*

The concentration of PAPS used was 0.4 mM.
The K_m is in μM.
The V_{max} is expressed as pmol substrate sulfated/min/mg protein.
Values shown are mean ± S.D., n = 3.
* Male values significantly lower than female values, $P < 0.05$

Table 3-2. The apparent PAPS K_m and V_{max} values of sulfotransferase from both male and female American lobster antennal gland cytosols.

Substrate	Sex	K_m	V_{max}
Phenol	♂	7.5 ± 0.9*	10.7 ± 1.4
	♀	11.0 ± 0.6*	29.6 ± 16.0
ß-Naphthol	♂	9.0 ± 4.2*	77.0 ± 36.9*
	♀	62.2 ± 3.5*	254 ± 93*
3-OH BaP	♂	59.0 ± 32.1	47.8 ± 33.7
	♀	49.9 ± 10.2	69.4 ± 18.8

The K_m is in μM.
The V_{max} is expressed as pmol/min/mg protein.
The concentration of phenolic substrates used were: 52 μM phenol, 300 μM ß-naphthol and 50 μM 3-OH BaP.
Mean ± S.D., n = 3, except ß-naphthol: male n = 5.
* Male values significantly lower than female values, $P < 0.05$

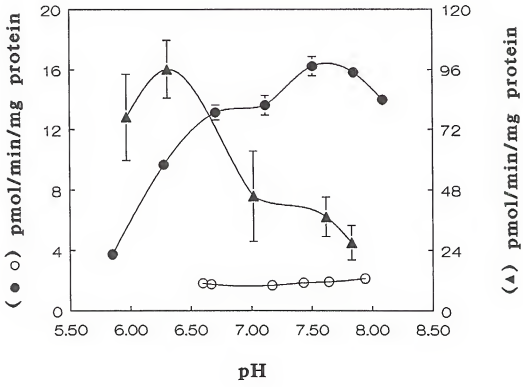

Figure 3-1. The pH profile of male aryl sulfotransferase. Assay conditions were described in "Method and Materials" section. Tubes contained 7.6 μM phenol (○), 6.6 μM ß-naphthol (●) or 10 μM 3-OH BaP (▲).

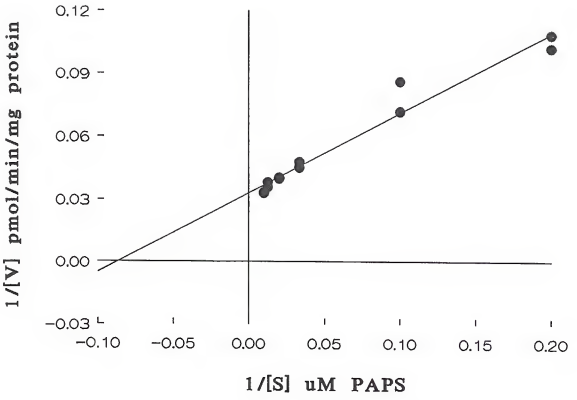

Figure 3-2. A typical Lineweaver-Burk plot for the determination of the PAPS K_m of aryl sulfotransferase in female. The assay condition were described in "Methods and Materials" section. Tubes contained 52 μM phenol.

account for 0.57 ± 0.13% body weight (mean ± S.D., n = 11) in gonadally regressed females (James, unpublished observations). Three female lobsters shown histologically to be in intermolt had very similar apparent K_ms of PAPS with ß-naphthol as substrate (data shown in Table 3-2).

UDP-glucosyltransferase

No UDP-glucuronyltransferase activities were observed with the three phenolic compounds used in this study. The pH optima observed for hepatopancreatic and antennal gland UDP-glucosyltransferases (UDPGTs) were 10.5 and 7.6 with ß-naphthol as substrate (Figure 3-3). Comparable results were observed for phenol. For 3-OH BaP, similar pH optima were observed for UDPGTs from hepatopancreas and antennal gland, the pH optima being 9.2 and 9.5, respectively. The pH optima for HP UDPGT were all in the alkaline range and were 10.2, 10.5 and 9.2 for phenol, ß-naphthol and 3-OH BaP, respectively.

Freezing and thawing of hepatopancreas microsomes resulted in a 15% increase in UDPGT activity. When microsomes were solubilized with the non-ionic detergent, Lubrol PX, at a final concentration of 0.05% (W/V) in the assay, there was a 45 - 69% increase in the UDPGT activity over the fresh microsomes. The apparent K_m and V_{max} values of UDPGT from hepatopancreas for different phenolic substrates are tabulated in Table 3-3. The apparent K_m and V_{max} of UDP-glucose with different phenolic substrates are tabulated in Table 3-4. The hepatopancreatic UDPGT had the lowest K_m and V_{max} with 3-OH

BaP. Phenol had very low affinity (K_m 1300 - 1600 μM) for hepatopancreatic UDPGT (Table 3-3). The UDP-glucose apparent K_m values were all in the 10^{-4} M concentration range, and were usually an order of magnitude higher than the apparent K_m values for PAPS (Tables 3-2 and 3-4).

The antennal gland UDPGT had the highest V_{max} with 3-OH BaP and the lowest with phenol. Phenol had the highest K_m (1200 - 2100 μM) and the K_ms with ß-naphthol and 3-OH BaP were similar (Table 3-5). The pH optimum for antennal gland UDPGT was similar to that found in hepatopancreas for 3-OH BaP (9.5) but was considerably lower for phenol and ß-naphthol (7.6).

Purification of antennal gland aryl sulfotransferases

Aryl sulfotransferases from male and female American lobsters antennal gland cytosolic fractions were partially purified by DEAE-cellulose anion exchange column. The results are shown in Figures 3-4 and 3-5. The partially purified male aryl sulfotransferase fractions 29-35, 36-42, 43-48 and 61-68 were further purified by PAP agarose affinity column. For females, fractions 13-20, 40-50 and 65-70 were used. The results from female fractions 40-50 purified by PAP agarose affinity column are illustrated in Figure 3-6. All samples were subjected to SDS-PAGE analysis with silver stain detection. For female fractions 40-50 purified by PAP agarose affinity column, the SDS-PAGE results are shown in Figure 3-7. The other samples were too dilute for SDS-PAGE detection.

Table 3-3. The apparent K_m and V_{max} values of UDP-glucosyltransferase from both male and female American lobster hepatopancreas for different substrates.

Substrate	Sex	pH Optimum	K_m	V_{max}
Phenol	♂	10.2	1300 ± 1000	555 ± 434
	♀	10.2	1600 ± 600	1350 ± 720
ß-Naphthol	♂	10.5	58.9 ± 4.8	965 ± 288
	♀	10.5	89.5 ± 30.3	1040 ± 614
3-OH BaP	♂	9.2	13.1 ± 4.5	77 ± 57
	♀	9.2	11.0 ± 2.2	82 ± 51

The concentration of UDP-glucose used was 2.6 mM.
The K_m is in μM.
The V_{max} is expressed as pmol glucoside formed/min/mg protein.
Mean ± S.D., n = 3.

Table 3-4. The apparent K_m and V_{max} values of UDP-glucosyltransferase from both male and female American lobster hepatopancreas for UDP-glucose with different substrates.

Substrate	Sex	K_m	V_{max}
Phenol	♂	428 ± 130	982 ± 363*
	♀	482 ± 143	1530 ± 242*
ß-Naphthol	♂	283 ± 33.0	557 ± 156
	♀	255 ± 53.5	642 ± 141
3-OH BaP	♂	693 ± 178*	70.3 ± 9.0
	♀	393 ± 56.3*	63.6 ± 6.3

The K_m is in μM.
The V_{max} is expressed as pmol glucoside formed/min/mg protein.
The concentration of substrate used: 5 mM phenol, 500 μM ß-naphthol and 16 μM 3-OH BaP.
Mean ± S.D., n = 3.
* $P < 0.05$ Male versus female for the same substrate.

Table 3-5. The apparent K_m and V_{max} values of UDP-glucosyltransferase from both male and female American lobster antennal glands for different substrates.

Substrate varied	Sex	pH Optimum	K_m	V_{max}
Phenol	♂	7.6	1,230	86.5
	♀		2,110	480
UDPG	♂	--	520	260
	♀		751	389
ß-Naphthol	♂	7.6	15.8	1,050
	♀		8.5	592
UDPG	♂	--	134	412
	♀		116	291
3-OH BaP	♂	9.5	12.5	1,390
	♀		9.1	1,310
UDPG	♂	--	583	1,080
	♀		510	1,330

The K_m is in μM.
The V_{max} is expressed as pmol/min/mg protein.
The concentration of substrate used: 2.6 mM UDP-glucose for substrate K_m studies 5 mM phenol, 52.8 μM ß-naphthol and 16 μM 3-OH BaP for UDPG K_m studies.
Pools of microsomes from three animals were used for each sex.

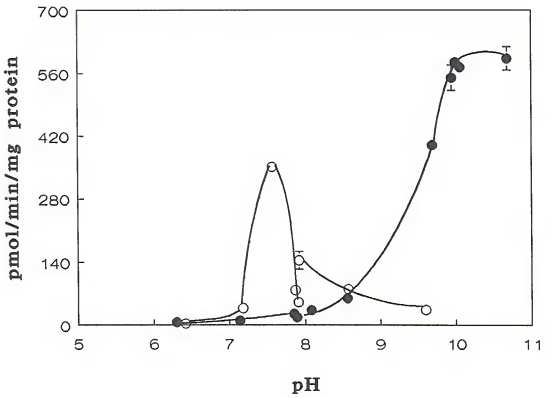

Figure 3-3. The pH profile of hepatopancreas and antennal gland UDP-glucosyltransferases using ß-naphthol as acceptor. For hepatopancreas UDPGT (●), 19 μM ß-naphthol was used and 11 μM for antennal gland UDPGT (○). 0.5 M sodium phosphate buffers ranging from pH 5.5 to 8.5 and 0.5 M glycine-sodium hydroxide buffers ranging from pH 8.5 to 12.7 were used in the assays.

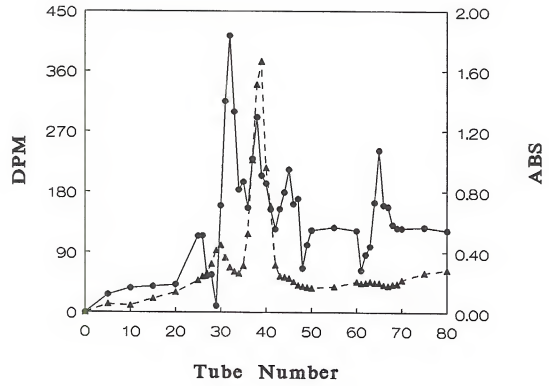

Figure 3-4. DEAE-cellulose chromatography of 150,000*g* male antennal gland supernatant solution. Assay conditions were described in "Methods and Materials" section. Tubes contained 7.6 μM [^{14}C]-phenol. ●: dpm, ▲: UV absorption at 280 nm.

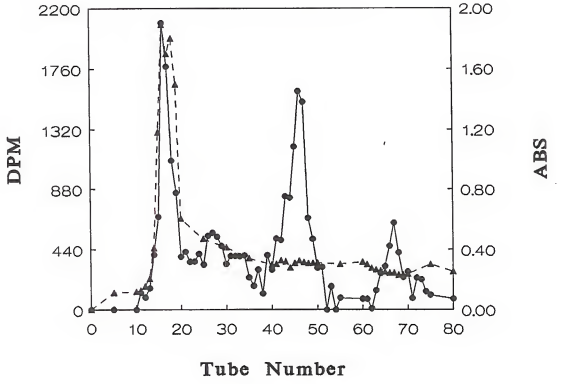

Figure 3-5. DEAE-cellulose chromatography of 150,000*g* female antennal gland supernatant solution. Assay conditions were described in "Methods and Materials" section. Tubes contained 7.6 μM [^{14}C]-phenol. ●: dpm, ▲: UV absorption at 280 nm.

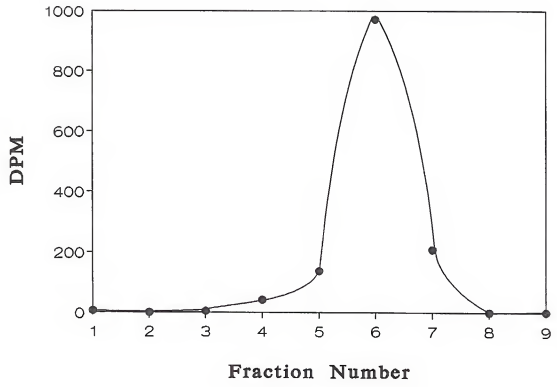

Figure 3-6. PAP-agarose affinity column chromatography of female DEAE-cellulose column eluent fractions 40-50. Assay condition was described in "Methods and Materials". Each tube contained 20 μl purified enzyme and 5.97 μM [^{14}C]-phenol.

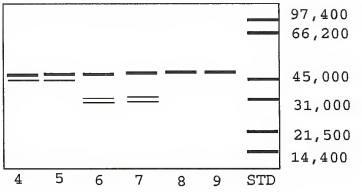

Figure 3-7. Schematic of female fractions 40-50 from DEAE chromatograph column further purified by PAP-agarose affinity column fractions 4-9 SDS-PAGE gel with silver stain detection.

Discussion

Aryl sulfotransferase

Phenol sulfotransferase activity was found in antennal gland cytosolic fraction, but not hepatopancreas cytosolic fraction. This was similar to findings in the spiny lobster (Schell and James, 1989), but differed from the results of Elmamlouk and Gessner (1978) who found 4-nitrophenol sulfotransferase activity in the hepatopancreas of the American lobster. It was possible that sulfotransferase was present in the intact hepatopancreas cells, but was masked by sulfatase activity that was released from the endoplasmic reticulum by homogenization. High sulfatase activity has been found in spiny lobster hepatopancreas cytosol and microsomes (James, unpublished). *In vivo* studies with fenitrothion-exposed blue crabs showed that sulfatase treatment of polar metabolites of fenitrothion found in the hepatopancreas yielded 3-methyl-4-aminophenol and 3-methyl-4-nitrophenol, suggesting that sulfate conjugates of these metabolites were produced in the crab hepatopancreas (Johnson and Corbett, 1986).

The K_m for the antennal gland phenol sulfotransferase was in the μM range and was lower in males, 11.6 μM, than females, 22.4 μM (see Table 3-1). Reported K_ms for phenol sulfotransferase in mammalian species (reviewed by Roy, 1981) range from 40 μM in rat brain and 70 μM in ox kidney to 1800 μM in rat liver and 2500 μM in guinea pig liver. The K_ms for ß-naphthol and 3-OH BaP (Table 3-1) were similar to the K_ms for these substrates in the spiny lobster, 36 μM, although the V_{max} values for ß-naphthol and 3-OH BaP were much higher in the

spiny lobster (Schell and James, 1989). The ß-naphthol K_m was also similar to that reported for rat liver sulfotransferases I and II (Roy, 1981). The pH optima for the antennal gland sulfotransferases were similar to those reported for aryl sulfotransferases I and II (Sekura and Jakoby, 1979). Phenol, naphthol and 3-OH BaP sulfotransferase activities have not previously been measured in crustacean species, although it is known that sulfate conjugates of naphthol are formed by adult and larval shrimp exposed to naphthalene (Sanborn and Malins, 1980).

The PAPS K_m values were lowest for phenol and for males with ß-naphthol, 7.5 - 11 μM, and were about five times higher for 3-OH BaP and females with ß-naphthol, 50-62 μM (see Table 3-2). Although the PAPS K_m for females with ß-naphthol as acceptor substrate showed little variability in gonadally regressed, intermolt lobsters (Table 3-2), studies with lobsters in various molt stages, and varying degrees of gonadal maturation suggested that physiological changes associated with molting affected the PAPS K_m values. Changes with molt cycle status may be expected in lobsters. Snyder and Chang (1991) showed that ecdysone was metabolized differently by female lobsters, depending on molt stage. The K_m studies and the differing pH optima found for sulfotransferase with different substrates suggest that more than one sulfotransferase enzyme is present in the antennal gland. Preliminary purification studies showed that at least three phenol sulfotransferase peaks could be isolated by DEAE-chromatography from female antennal gland cytosol. It is possible that ecdysone, 20-hydroxyecdysone or other molting

hormones or factors may regulate the synthesis and properties of the sulfotransferases in the lobster, and this deserves further study.

Carbohydrate conjugation

There was no evidence of UDP-glucuronosyltransferase activity in hepatopancreas microsomes with any of the phenolic substrates studied. This agreed with the findings of Elmamlouk and Gessner (1978) who were unable to find p-nitrophenol glucuronosyltransferase activity in the American lobster, and findings in the spiny lobster (Schell and James, 1989). UDP-glucosyltransferase activity was found in lobster hepatopancreatic and antennal gland microsomes with all three substrates (Tables 3-3 , 3-4 and 3-5). Dutton (1981) also suggested that invertebrates form glucoside conjugates and vertebrates glucuronide conjugates.

Mammalian and fish UDP-glucuronosyltransferases are found on the lumen of the endoplasmic reticulum, and maximal activity may be measured only after mechanical (freezing and thawing, sonication) or chemical (non-ionic detergent) disruption of the microsomes (Burchell and Coughtrie, 1989; Clarke *et al.*, 1991). Studies of the latency of invertebrate UDP-glucosyltransferases have not given clear results. In the present study, activity was increased by both freezing and thawing and treatment with Lubrol PX. In the housefly, Triton X-100 was reported to stimulate glucosidation of 4-nitrophenol (Morello and Repetto, 1979), whereas in the fruit fly, Triton X-100 inhibited glucosidation of xanthurenic acid (Real and Ferré, 1990). In a previous study with the spiny lobster,

freezing and thawing caused some increase in activity but treatment with Lubrol PX did not affect UDP-glucosyltransferase activity (Schell and James, 1989).

Very different K_m values were found with the three different acceptor substrates. Phenol was a poor substrate, having a high K_m in both antennal gland and hepatopancreas microsomes (Tables 3-3 and 3-5). The K_m values for ß-naphthol glucosyltransferase were in the μM range and were lower in the antennal gland than the hepatopancreas. There was no obvious sex difference in ß-naphthol K_m in either organ, although the results showed considerable individual variability in the ß-naphthol K_m and V_{max} in hepatopancreatic microsomes, especially in females (Table 3-3). Also of interest was the switch in pH optimum between hepatopancreas (10.2-10.5) and antennal gland (7.6) for both phenol and ß-naphthol. The hepatopancreas pH optima are very high and outside the usual physiological range. The pH optimum was higher than that found by Elmamlouk and Gessner (1978) for p-nitrophenol glucosidation in the American lobster (pH 7.9-8.1). In the spiny lobster, however, the pH optimum for 4-methylumbelliferone glucosyltransferase was greater than 8.5 (Schell and James, 1989) and the pH optimum for ß-naphthol glucosyltransferase was 9.8 in the fruit fly (Real *et al.*, 1991). The differences in pH optima between organs suggests that more than one form of glucosyltransferase is present in the American lobster, with tissue-specific expression. The K_m for 3-OH BaP glucosyltransferase was very low (9-13 μM) in both antennal gland and hepatopancreas, but V_{max} was considerably higher in antennal gland than hepatopancreas (Tables 3-3 and 3-5).

Unlike ß-naphthol and phenol, the pH optima for 3-OH BaP glucosyltransferase activities in antennal gland and hepatopancreas were very similar (9.2-9.5). This suggests that the same form of 3-OH BaP glucosyltransferase is present in both organs, but that there is more enzyme in the antennal gland.

The UDP-glucose K_m values were in the high μM range for all substrates and both organs, and were always higher than the PAPS K_m values. This is similar to what is found for the UDP-glucuronic acid K_m values in mammals, which are normally much higher than PAPS K_m values for the same substrates (Mulder, 1982). UDP-glucose K_m values were highest with phenol and 3-OH BaP as acceptor substrates, although for 3-OH BaP the UDP-glucose K_m in hepatopancreas was lower in females than males (Table 3-4). With ß-naphthol as substrate, the UDP-glucose K_m was lower in antennal gland than hepatopancreas (Tables 3-4 and 3-5). Since the ß-naphthol glucosyltransferase K_m was also lower in antennal gland than hepatopancreas (Tables 3-3 and 3-5) and lower than the ß-naphthol sulfotransferase K_m (Table 3-1), this suggests that glucosidation may be a major pathway for ß-naphthol conjugation in the antennal gland, especially in females where the PAPS K_m was much higher than that in males (Table 3-2). This was borne out by *in vivo* studies (*vide infra*).

These studies showed that there were sex differences in several parameters related to sulfate and glucoside conjugation in the lobster. Sex differences in the conjugation of phenolic compounds have been previously reported in rats. Female rats dosed with acetaminophen (Smith

and Griffiths, 1976) and 2,6-dimethoxyphenol (Miller *et al.*, 1974) excreted less sulfate and more glucuronide conjugates in urine than males. The present studies suggest that there will be differences between male and female American lobsters in the conjugation of ß-naphthol and possibly 3-OH BaP.

Purification of antennal gland aryl sulfotransferases

As mentioned in Chapter 1, there are multiple forms of aryl sulfotransferase and UDP-glucosyltransferase present in many species studied. Present studies show that this is true for the American lobster. Results from DEAE-cellulose anion exchange chromatography indicated that there were four phenol sulfotransferase isozymes in male antennal gland and three in female. Due to low percentage yield and the protocol used, homogeneity of the enzymes of interest was not achieved in this study. More antennal gland cytosolic fractions are needed for future study and gel filtration chromatography (i.e. Sephacryl S-200) should be used after DEAE-cellulose anion exchange chromatography and before PAP-agarose affinity chromatography (Falany *et al.*, 1990). Results of SDS-PAGE for one partially purified phenol sulfotransferase from female antennal gland showed that the molecular weight of this isozyme might be either 30,000 or 32,000 daltons (Figure 3-7). One form of human liver phenol sulfotransferase exists *in vivo* as a homodimer with an apparent molecular size of 68,000 daltons as determined by Sephacryl S-200 with a subunit of 32,000 daltons as determined by SDS-PAGE (Falany *et al.*, 1990).

For future studies, purification protocols need to be established in order to obtain the physical properties of all isozymes and produce antibodies for all isozymes to screen any inducer or repressor from environmental contaminants. As mentioned above, the molt cycle of the American lobster affected the PAPS K_m values and it will be interesting to see how each isozyme is expressed and regulated in different molt stages.

In Vivo Studies

Results

Elimination of phenolic compounds from hemolymph

The elimination of intrapericardially injected [^{14}C]-phenol was found to be dose-dependent in male and female adult lobsters. Phenol was well separated from its glucoside and sulfate conjugates by XAD-2 minicolumn chromatography, with 99.9% of phenol standard retained by the column and eluted in the chloroform fraction, while 99% of the phenyl sulfate or phenyl glucoside passed through the column with the ammonium chloride buffer. After a single 0.1- or 0.2-mg/kg dose of [^{14}C]-phenol, the concentration of parent phenol in hemolymph declined very rapidly (Figure 3-8 shows data from the 0.2-mg/kg dose), such that by 1 hour after the dose, parent phenol was undetectable (< 0.5 ng/ml) in hemolymph. The pharmacokinetic parameters for elimination of phenol from hemolymph are presented in Table 3-6. The rapid decline in hemolymph phenol concentration was not apparent by examining total radioactivity in hemolymph, which remained constant between 10 minutes and 4 to 6 hours after the dose and then

declined slowly. The slow decline in total radioactivity was due to the slow elimination of phenyl sulfate from hemolymph.

A similar XAD-2 minicolumn chromatography protocol was used with modification for ß-naphthol. An aliquot of 10 ml of a mixture of acetone/0.1 M ammonia buffer, pH 10, 3:7, was used to elute the column instead of 1 ml acetone. The XAD-2 minicolumns retained 98% ß-naphthol and ß-naphthyl glucoside, while the ß-naphthyl sulfate was not retained by the column. ß-Naphthyl glucoside was eluted from the column by mixture of acetone/0.1 M ammonia buffer, pH 10, 3:7, and ß-naphthol was eluted in the chloroform/methanol, 3:1, fraction.

Results from HPLC analyses and enzymatic hydrolyses of the acetonitrile extracts showed that [^{14}C]-ß-naphthol was rapidly metabolized to sulfate and glucoside conjugates. Results from *in vitro* studies conducted at 12.5°C (the normal temperature of sea water in lobster holding tanks) showed that the conjugating enzymes had similar K_ms but very low V_{max}s compared to those measured at 35°C. For hepatopancreatic ß-naphthol UDP-glucosyltansferases measured at 35°C the K_m was 89.5 ± 30.3 μM and V_{max} 1040 ± 614 pmol/min/mg protein (Table 3-3), when measured at 12.5°C the K_m was 83.1 μM and the V_{max} was 322 pmol/min/mg protein. The mean K_m values and lowest V_{max} values for ß-naphthol UDP-glucosyltransferase and ß-naphthol sulfotransferase measured at 35°C were used as constants in Model B to fit the data. The disappearance of ß-naphthol is shown in Figure 3-9.

The parameters estimated from the pharmacokinetic models are summarized in Tables 3-7 and 3-8. For ß-naphthol, the

Table 3-6. Pharmacokinetic parameters for elimination of phenol from hemolymph following an intrapericardiac dose.

Parameter	Units	Mean ± S.D. (N = 4)
Half-life, α	min	8.74 ± 0.02
Half-life, β	min	14.00 ± 0.03
Whole body clearance	$ml \times min^{-1} \times kg^{-1}$	28.10 ± 2.09
Intercompartment clearance	$ml \times min^{-1} \times kg^{-1}$	28.40 ± 5.70
V_c[1]	$ml \times kg^{-1}$	204 ± 19.3
V_p[2]	$ml \times kg^{-1}$	145 ± 28.7

A two-compartment model was fit to the data. The dose of phenol was 0.12 to 0.22 mg/kg and values were normalized to 0.2 mg/kg before fitting the data.

1. V_c is the volume of the central compartment.
2. V_p is the volume of the peripheral compartment.

Table 3-7. Pharmacokinetic parameters estimated from Model A for elimination of ß-naphthol from hemolymph following an intrapericardiac dose.

Parameter	Units	Sex	Mean ± S.D. (N = 4)
Half-life, α	min	♂	26 ± 19
		♀	29 ± 15
Half-life, ß	h	♂	63.9 ± 30.9*
		♀	30.6 ± 6.8*
V_c[1]	$ml \times kg^{-1}$	♂	297 ± 69**
		♀	342 ± 94**
V_p[2]	$ml \times kg^{-1}$	♂	560 ± 160**
		♀	780 ± 200**
Whole body clearance	$ml \times h^{-1} \times kg^{-1}$	♂	11.1 ± 5.9*
		♀	26.4 ± 6.5*
Intercompartment clearance	$ml \times h^{-1} \times kg^{-1}$	♂	553 ± 532
		♀	498 ± 503
k_{12}	h^{-1}	♂	1.7 ± 1.3
		♀	1.4 ± 1.0
k_{21}	h^{-1}	♂	0.48 ± 0.34
		♀	0.58 ± 0.43
k_{10}	h^{-1}	♂	0.037 ± 0.014*
		♀	0.080 ± 0.019*

1. V_c is the volume of the central compartment.
2. V_p is the volume of the peripheral compartment.
* Male values are significantly lower or slower than female values, $P < 0.05$.
** The volumes of the central compartment are significantly lower than the volumes of the peripheral compartment, $P < 0.05$

Table 3-8. Pharmacokinetic parameters estimated from Model B for formation and elimination of ß-naphthol metabolites from hemolymph following an intrapericardiac dose.

Parameter	Units	Sex	Mean ± S.D. (N = 4)
Half-life of ß-naphthyl glucoside	h	♂	28.4 ± 20.6
		♀	10.4 ± 3.7
Half-life of ß-naphthyl sulfate	h	♂	3.3 ± 1.6
		♀	4.3 ± 1.7
Half-life of ß-naphthyl glucoside[1]	h	♂	51.2
		♀	28.9
Half-life of ß-naphthyl sulfate[1]	h	♂	7.8
		♀	9.4
k_{12}	h^{-1}	♂	2.4 ± 2.5
		♀	1.3 ± 1.3
k_{21}	h^{-1}	♂	1.3 ± 1.3
		♀	0.58 ± 0.56
k_{gn}[2]	h^{-1}	♂	0.20 ± 0.019*
		♀	0.040 ± 0.0029*
V_c[3]	$ml \times kg^{-1}$	♂	258 ± 55
		♀	327 ± 74

1. Manually estimated from a log linear plot of concentration versus time.
2. k_{gn} is the rate constant for ß-glucosidase.
3. V_c is the volume of the central compartment.

* Male values are significantly higher than female values, $P < 0.05$.

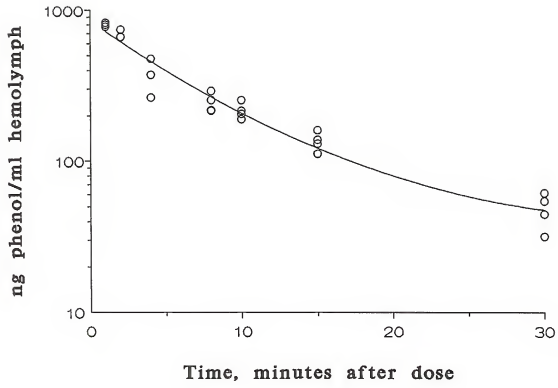

Figure 3-8. Elimination of unchanged phenol from hemolymph. Values shown are four lobsters dosed (mixed sex) with 0.2 mg/kg (normalized). Hemolymph was analyzed for phenol as described in the "Materials and Methods" section.

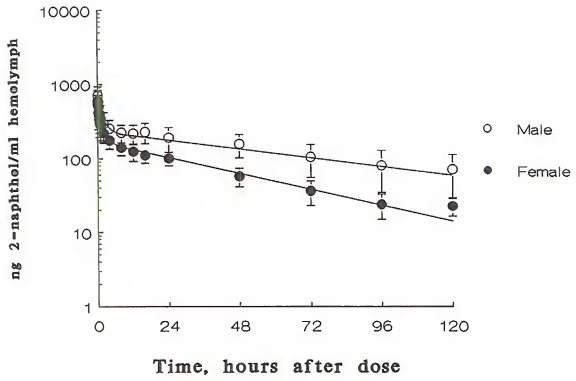

Figure 3-9. Elimination of ß-naphthol from hemolymph of the American lobsters. Animals were intrapericardially dosed with 0.25 mg/kg of ß-naphthol. Values shown are mean ± S.D., n = 4.

half-lives estimated by Model A for distribution phase, α, were very similar for both males, 26 ± 19 min (mean ± S.D., N = 4), and females, 29 ± 15 min, but elimination phase half-lives, ß, in males, 63.9 ± 30.9 h, were longer than in females, 30.6 ± 6.8 h (Table 3-7)($P < 0.05$). For both males and females, the volumes of the central compartment were significantly lower those of the peripheral compartment ($P < 0.05$). The males, 11.1 ± 5.9 $ml \times h^{-1} \times kg^{-1}$, had lower whole body clearance than the females, 26.4 ± 6.5 $ml \times h^{-1} \times kg^{-1}$ (Table 3-7)($P < 0.05$). The rate constants k_{10} of males estimated from Model A, 0.037 ± 0.014 h^{-1}, were significantly lower those for females, 0.080 ± 0.019 h^{-1} ($P < 0.05$). Although the estimated values for the central compartment, V_c were similar in Models A and B, Model B did not provide a good fit for the data.

Elimination of the phenolic compounds metabolites from hemolymph

Analysis of hemolymph extracts by XAD-2 minicolumn chromatography showed that phenol was converted rapidly to material that was not retained by the XAD-2 resin. HPLC of hemolymph acetonitrile extracts showed that > 99% of the [^{14}C] in hemolymph at 1, 2 and 24 hours was a single polar metabolite that co-migrated with the major urinary metabolite. The elimination of this metabolite from hemolymph was much slower (overall $t_{1/2}$ of 6.3 hours for males and 11.9 hours for females, Figure 3-10) than the elimination of phenol (Figure 3-8). Type V arylsulfatase, 1.2 units, hydrolyzed 30% of the hemolymph metabolite (100 ng phenol equivalents) to phenol in 24 hours. Under the same incubation conditions, type V

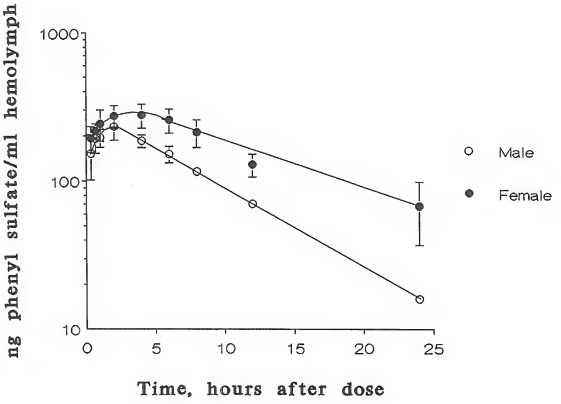

Figure 3-10. Elimination of the major metabolite of phenol from hemolymph of male and female lobsters. Lobsters were dosed intrapericardially with 0.1 mg/kg phenol. Values shown are mean ± S.D. for three male or female lobsters.

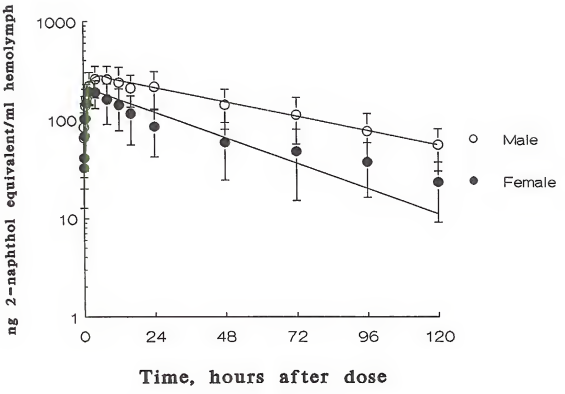

Figure 3-11. The hemolymph concentration of ß-naphthyl glucoside in the American lobsters. Animals were intrapericardially dosed with 0.25 mg/kg of ß-naphthol. Values shown are mean ± S.D., n = 4. The slope of line was estimated from Rstrip® software.

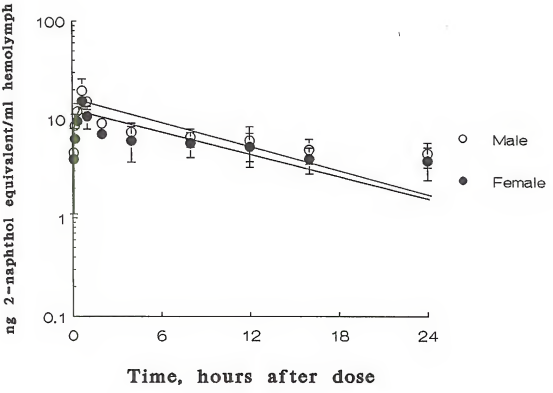

Figure 3-12. The hemolymph concentration of ß-naphthyl sulfate in the American lobsters. Animals were intrapericardially dosed with 0.25 mg/kg of ß-naphthol. Values shown are mean ± S.D., n = 4. The slope of line was estimated from Rstrip® software.

arylsulfatase hydrolyzed 50% of a 0.1-mM solution of *p*-nitrophenyl sulfate to *p*-nitrophenol.

For ß-naphthol, sulfate and glucoside conjugates were formed *in vivo*. The half-life of ß-naphthyl glucoside formed *in vivo* estimated from Model B was 28.4 ± 20.6 h for males and 10.4 ± 3.7 h for females (Table 3-8). The half-lives of ß-naphthyl sulfate were 3.3 ± 1.6 h and 4.3 ± 1.7 h for males and females, respectively (Table 3-8). The rate constants of ß-glucosidase, k_{gn}, were significantly higher in males, 0.20 ± 0.019 h^{-1}, than those in females, 0.040 ± 0.0029 h^{-1} ($P < 0.05$). ß-Naphthol and its metabolites were very slowly eliminated from lobster hemolymph at similar rates. Manual estimation of the terminal elimination phase $t_{1/2}$ of ß-naphthyl sulfate, using a log linear plot of concentration versus time showed that the males had a half-life of 7.8 h and the females 9.4 h (Figure 3-12). For ß-naphthyl glucoside, the terminal elimination phase $t_{1/2}$ was 28.9 h for the females and 51.2 h for the males (Figure 3-11).

Tissue distribution of radioactivity

In studies with [^{14}C]-phenol, groups of lobsters were dissected at 30 minutes, 4 hours and 24 hours after the 0.1 mg/kg dose, and all tissues were analyzed for total radioactivity. For studies with ß-naphthol, lobsters were intrapericardially injected with 0.25 mg/kg [^{14}C]-ß-naphthol either 1 day or 5 days before dissection. The percentage of dose in each tissue was calculated by assaying samples for radioactivity and correcting for the total tissue weight. Mean weights of hemolymph, muscle, shell and shell membrane as

a percentage of body weight were 21.8, 40.5, 22 and 6 (Barron *et al.*, 1988). The results are shown in Figure 3-13 through Figure 3-16 and Tables 3-9 and 3-10.

For both phenol and ß-naphthol, negligible amounts of [^{14}C] were found in stomach, intestine, intestinal contents or gonads at any time point, so these data are not shown separately, but the total amount in these tissues is included in the whole animal percentage of dose recovered value. At all times, the tissue with the highest concentration of radioactivity was the antennal gland, although for ß-naphthol hepatopancreas also had high concentrations (Figure 3-13 through Figure 3-16). For phenol, 2.0% of the dose remained in tissues of males after 24 hours and 8.1% in females (Table 3-9), but for ß-naphthol much more the dose was retained at 24 hours, 41.2% for males and 18.3% for females (Table 3-10).

For phenol, at 4 and 24 hours after the dose, urine contained the highest concentration of radioactivity (Figures 3-13 and 3-14), suggesting that urinary excretion was a major route of elimination. The percentage of dose found in urine dose not represent total urinary excretion at any time point, as we were able to collect only what was present in the bladders at time of sacrifice. At 30 minutes after a 0.1-mg/kg dose, only 60.7% of the dose was found in all tissues and 0.4% was found in the terminal urine sample. This suggested that a large percentage of the phenol dose was being rapidly excreted into the tank water, presumably across the gills.

For ß-naphthol, two female lobsters were externally cannulated from the nephropores to collect total urine. By 5

Table 3-9. Distribution of [^{14}C] after intrapericardiac injection of phenol (0.1 mg/kg) to lobster, *Homarus americanus*.

	Males			Females	
	30 min	4 h	24 h	4 h	24 h
			% dose recovered		
Hemolymph	22.6 ± 2.8	16.3	2.0 ± 0.2	22.2 ± 5.4	8.1 ± 3.7
Muscle	23.4 ± 11.5	7.7	1.9 ± 0.2	8.6 ± 0.3	3.7 ± 0.5
Shell	5.6 ± 0.9	6.4	1.7 ± 0.05	9.4 ± 1.5	4.4 ± 0.5
Antennal gland	0.3 ± 0.1	0.5	0.1 ± 0.0	1.8 ± 1.0	0.3 ± 0.1
Urine	0.4 ± 0.1	14.6	4.3 ± 0.3	12.3 ± 9.2	11.9 ± 0.9
Hepatopancreas	3.6 ± 1.1	1.6	0.5 ± 0.1	2.0 ± 0.4	2.0 ± 0.1
Gill	1.9 ± 0.2	1.6	0.2 ± 0.05	2.2 ± 1.1	0.9 ± 0.7
Whole animal excluding urine	60.7 ± 6.5	34.6	25.7 ± 8.7	42.5 ± 7.6	11.5 ± 1.8

All values are mean ± S.D., N = 3 except 4 hours male, N = 1.

Table 3-10. Distribution of [^{14}C] after intrapericardiac injection of ß-naphthol (0.25 mg/kg) to lobster, *Homarus americanus*.

	Males		Females	
	1 day	5 days	1 day	5 days
	% dose recovered			
Hemolymph	41.2 ± 12.0	12.7 ± 6.1	18.3 ± 6.6	5.0 ± 1.9
Muscle	6.8 ± 1.0	2.9 ± 1.4	5.9 ± 1.7	1.7 ± 0.4
Shell	4.2 ± 0.6	0.9 ± 0.5	1.7 ± 0.6	0.6 ± 0.1
Antennal gland	0.4 ± 0.2	0.2 ± 0.1	0.3 ± 0.2	0.2 ± 0.2
Urine	0.6[1]	1.1 ± 0.6	0.6 ± 0.6	5.1 ± 7.0[2]
Hepatopancreas	6.8 ± 3.0	7.9 ± 3.1	9.0 ± 0.9	3.3 ± 0.7
Gill	2.0 ± 0.5	1.0 ± 0.4	1.5 ± 0.4	0.5 ± 0.2
Whole animal excluding urine	65.6 ± 10.7	28.5 ± 9.0	42.5 ± 7.6	12.5 ± 1.8

All values are mean ± S.D., N = 3 for 1 day, N = 4 for 5 days.

1. N = 2.
2. Two animals were externally cannulated from the nephropores to collect total urine.

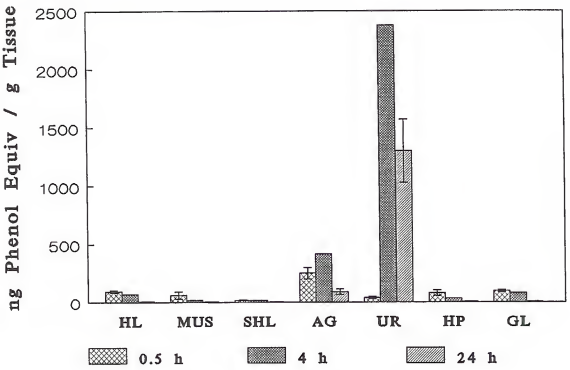

Figure 3-13. Tissue concentrations of [^{14}C] in male lobsters dosed intrapericardially with 0.1 mg/kg phenol. Values shown are mean ± S.D., N = 3 except 4-h male, N = 1. HL: hemolymph, MUS: muscle, SHL: shell, AG: antennal gland, UR: urine, HP: hepatopancreas, GL: gills.

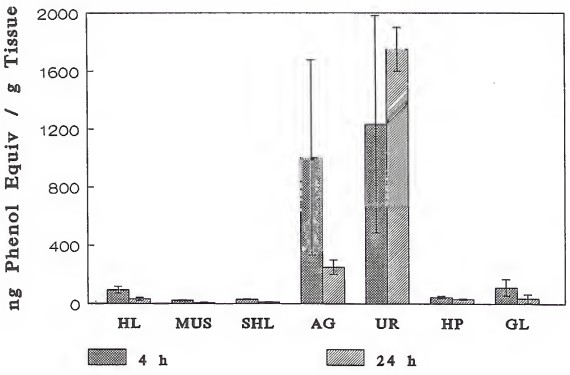

Figure 3-14. Tissue concentrations of [^{14}C] in female lobsters dosed intrapericardially with 0.1 mg/kg phenol. Values shown are mean ± S.D., N = 3. HL: hemolymph, MUS: muscle, SHL: shell, AG: antennal gland, UR: urine, HP: hepatopancreas, GL: gills.

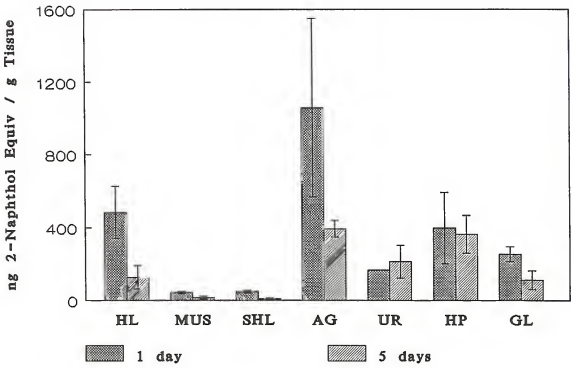

Figure 3-15. Tissue concentrations of [^{14}C] in male lobsters dosed intrapericardially with 0.25 mg/kg ß-naphthol. Values shown are mean ± S.D., N = 3 for 1-day lobsters, N = 4 for 5-day. HL: hemolymph, MUS: muscle, SHL: shell, AG: antennal gland, UR: urine, HP: hepatopancreas, GL: gills.

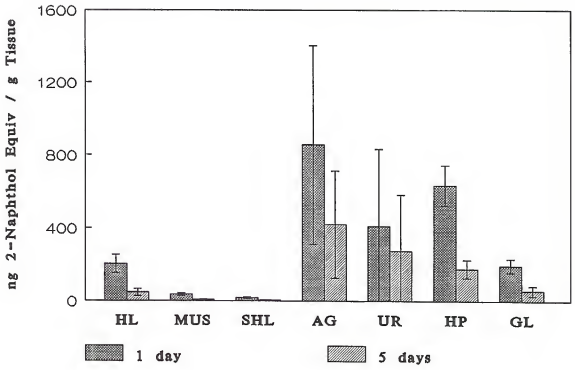

Figure 3-16. Tissue concentrations of [^{14}C] in female lobsters dosed intrapericardially with 0.25 mg/kg ß-naphthol. Values shown are mean ± S.D., N = 3 for 1-day lobsters, N = 4 for 5-day. HL: hemolymph, MUS: muscle, SHL: shell, AG: antennal gland, UR: urine, HP: hepatopancreas, GL: gills.

days after a 0.25-mg/kg dose, the percentages of dose excreted in urine were 3.1% and 15.5%. The total percentages of dose recovered in all tissues for those two animals, including urine, were 12.3% and 23.3%. As there was no evidence for feces being a major route of excretion, this suggested that, as in the case of phenol, the gills were involved in eliminating ß-naphthol and possibly its metabolite(s).

Branchial excretion

Tank water was analyzed for [^{14}C] at 30 minutes after the dose for individual lobsters. Lobsters were dosed with between 0.019 and 2.8 mg/kg [^{14}C]-phenol or between 0.048 mg/kg and 0.25 mg/kg [^{14}C]-ß-naphthol. The results for phenol are shown in Figure 3-16. For ß-naphthol, 7.7 ± 5.1% (mean ± S.D., N = 7) of the 0.25 mg/kg dose were excreted into the tank water in the first 30 minutes for males and 9.0 ± 5.3% for females. Two lobsters were dosed with different dosages and results showed that 13.1% of the 0.048 mg/kg dose and 1.46% of the 0.112 mg/kg dose were excreted into the tank water in the first 30 min. The branchially excreted materials were shown by extraction and HPLC analysis to consist primarily of parent compounds. For phenol, the importance of the branchial route increased with increasing dose, such that lobsters injected with greater than 2 mg/kg excreted over 90% of the dose through gills into tank water in the first 30 minutes (Figure 3-17).

One lobster dosed with 0.112 mg/kg of ß-naphthol was held in the tank for one hour, and similar amounts of radioactivity were found in the tank water at either the 30 min or 1 h

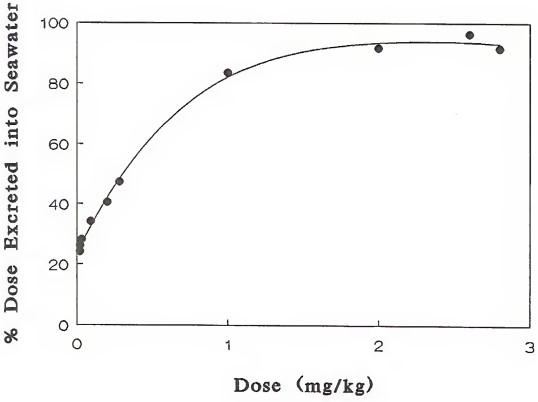

Figure 3-17. Total branchial excretion of [^{14}C]-phenol in the first 30 minutes after the dose. Lobsters were dosed with 0.019-2.8 mg/kg phenol. Each point represents an individual. The line drawn indicates a trend in the data.

period. In comparison with phenol, ß-naphthol was slowly excreted from the gills and the branchial route appeared to be less important in rapidly eliminating the parent compound. The rate constant of this process estimated from Model B was in 10^{-5} to 10^{-6} h^{-1} range.

Binding to hemolymph proteins

Measurement of protein binding by ultrafiltration of hemolymph collected 1 - 3 min after varying doses of phenol (0.05 - 2.0 mg/kg) showed that phenol was 93.5 ± 2.5% bound (mean ± S.D., N = 10) in the 0.1 - 5.5 µg/ml range. The radioactivity present in hemolymph collected 30 min after varying doses of phenol was 8 ± 2% bound: at this time less than 10% of the [^{14}C] present in hemolymph was parent phenol and greater than 90% was phenyl sulfate, showing that phenyl sulfate was not highly bound to hemolymph protein.

For 0.25 mg/kg ß-naphthol dosed female lobsters, 99.6 ± 0.2% (mean ± S.D., N = 4) of the dosed radioactivity were bound to the hemolymph protein 1 min after the dose, 90.4 ± 5.6% after 1 day and 84.6 ± 14.3% after 5 days. For males, 99.7 ± 0.1% of ß-naphthol-derived radioactivity were bound after 1 min, 96.4 ± 2.0% after 1 day and 94.2 ± 2.2% after 5 days. Thus, parent ß-naphthol (1 minute data) was greater than 99% protein bound. ß-Naphthyl glucoside, the major metabolite accounting for 39 to 60.6% of the hemolymph [^{14}C] at 1 day and 29.5 to 56.6% at 5 days, must also be greater than 93% protein bound. The extent of protein binding of the ß-naphthyl sulfate can not be determined as less than 4.5% of

the hemolymph radioactivity was the sulfate conjugate at 1 and 5 days.

Identification of the urinary metabolites

For phenol treated lobsters, urine contained high concentrations of [^{14}C] at 4 and 24 h after the dose. Analysis of urine by HPLC and radiochemical detection showed that the major urinary metabolite, comprising 97-99.5% of the urinary [^{14}C], was a polar compound that did not co-migrate with any of the known conjugates of phenol (Table 3-11). Small peaks, 0.1-3% of the urinary [^{14}C], co-migrated with phenyl glucoside standard. Later studies showed that if phenyl sulfate standard was dissolved in control lobster urine before HPLC analysis, the retention time matched that of the conjugates found in urine and hemolymph (Table 3-11).

Incubation of urine with 1 N HCl or 2 N HCl for 24 h converted part (1 N) or all (2 N) of the urinary [^{14}C] to phenol (Figure 3-18), indicating that only conjugates of phenol were present in urine. Incubation of urine with alkaline phosphatase and ß-glucuronidase did not alter the retention times of the urinary metabolites. Incubation of urine with ß-glucosidase resulted in the formation of small amounts of phenol, in accordance with the size of the phenyl glucoside peak. Incubation of urine with increasing amounts of type V arylsulfatase (1.2 to 6 units with 1 nmol conjugate) for 24 h resulted in the formation of increasing amounts of phenol, from 5 to 25% of the total [^{14}C]. Isolation of the metabolite from urine altered its susceptibility to hydrolysis by type V arylsulfatase. Very little (0-10%) of the

Table 3-11. Chromatographic separation of phenolic compounds and their conjugates by HPLC.

Compound	Retention time			
	A			B
	M1	M2	M3	
	min			
Phenyl phosphate	--	--	1.0	1.5
Phenyl sulfate	--	--	2.0	3.8
Phenyl sulfate in urine	--	--	2.8	4.7
Unknown metabolite[1]	--	--	2.8	4.8
Phenyl ß-D-glucuronide	--	--	4.6	5.4
Phenyl ß-D-galactoside	--	--	3.6	7.0
Phenyl ß-D-glucoside	--	--	4.0	9.0
Phenyl α-D-glucoside	--	--	--	11.8
Phenyl-N-acetyl-ß-D-glucosaminide	--	--	5.8	17.3
Phenol	--	--	10.4	17.6
Catechol	--	--	5.2	--
ß-Naphthyl sulfate	3.3	5.0	15.1	--
ß-Naphthyl glucoside	3.4	5.2	18.4	--
Urinary metabolite[2]	3.4	5.2	18.4	--
ß-Naphthol	13.5	29.7	--	--

A: The stationary phase was an Altex 5×0.45 cm Ultrasphere ODS column guard column coupled to a 25×0.45 cm analytical Ultrasphere ODS column.
M1: The mobile phase was 10 mM potassium phosphate, pH 2.75/acetonitrile (3:2 by volume).
M2: The mobile phase was 10 mM potassium phosphate, pH 2.75/acetonitrile (7:3 by volume).
M3: The mobile phase was 10 mM potassium phosphate, pH 2.75/acetonitrile (4:1 by volume).
B: The mobile phase was 10 mM potassium phosphate, pH 2.75/acetonitrile, 19:1, and the stationary phase was a Whatman ODS cartridge column, 15×0.45 cm.
1. From phenol treated lobster urine.
2. From ß-naphthol treated lobster urine.
All standards were dissolved in mobile phase for analysis.

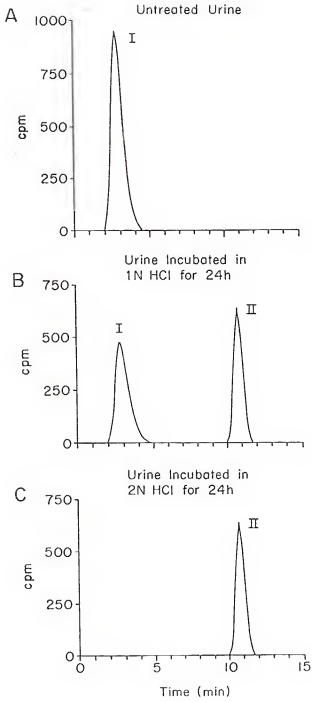

Figure 3-18. Acid hydrolysis of the major urinary metabolite of phenol excreted by lobsters.

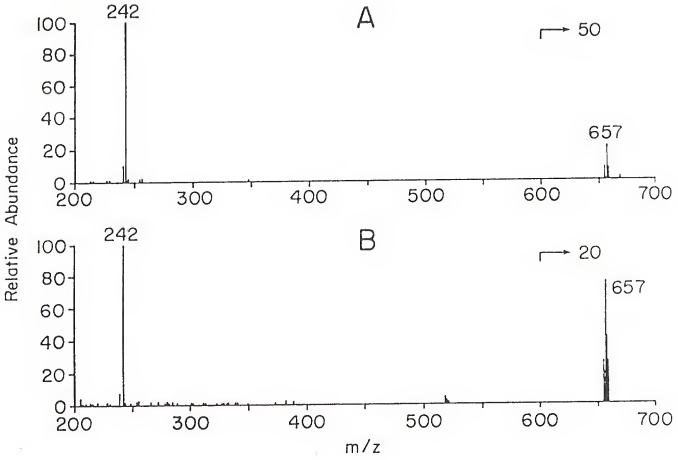

Figure 3-19. Positive ion pair FAB-mass spectra of the tetrabutylammonium ion pair of phenyl sulfate. Panel A is phenyl sulfate standard and the major urinary metabolite of phenol is in panel B. The signal at *m/z* 657 is due to two molecules of tetrabutylammonium and one molecule of phenyl sulfate.

radioactivity in dried and buffer-reconstituted acetone extract of evaporated urine was hydrolyzed to phenol by 1.2 to 6 units of type V arylsulfatase. Further purification of the acetone extract by Alumina N. Sep-Pak® chromatography resulted in a metabolite fraction that was completely hydrolyzed to phenol by 1.2 units of type V arylsulfatase. Incubation of urine or urine extracts with type VI arylsulfatase (0.14 units) resulted in complete hydrolysis of the conjugate to phenol.

To further confirm the identity of the conjugate, the FAB mass spectrum of the tetrabutylammonium ion pair of the isolated conjugate was measured. Figure 3-19 shows the positive ion mass spectrum of the tetrabutylammonium ion pair of standard phenyl sulfate and of the chromatographically isolated urinary metabolite.

For lobsters dosed with ß-naphthol, HPLC analysis of day-five urine showed that the major urinary metabolite, comprising 90-97.5% of the urinary [^{14}C], co-migrated with ß-naphthyl glucoside (Table 3-11). Small peaks, 2-9.7% of the excreted [^{14}C], co-migrated with ß-naphthyl sulfate. Incubation of urine with 2 N HCl (24 h) or 6 N HCl (6 h) converted part (2 N) or all (6 N) of the excreted [^{14}C] to ß-naphthol which indicated that only conjugates of the parent compound were present in urine. Incubation of urine with type VI arylsulfatase (0.14 units) resulted in the formation of small amounts of ß-naphthol, in accordance with the size of the ß-naphthyl sulfate peak.

Incubation of urine with ß-glucosidase (7.8 units) for 24 h resulted in partial hydrolysis (5.7-15% of the total [^{14}C])

of the major urinary metabolite. Isolation of the major urinary metabolite by HPLC chromatography resulted in completely hydrolysis of the conjugate to ß-naphthol by ß-glucosidase (7.8 units).

Properties of chemically and enzymatically synthesized sulfate conjugates

The enzymatically synthesized phenyl sulfate from rat cytosolic fraction had the same retention time (2.8 min, Table 3-11) as that of the major urinary metabolite from phenol-dosed lobster urine and phenyl sulfate standard dissolved in control lobster urine before HPLC analysis. The chemically synthesized phenyl sulfate sodium salt (by the method of Burkhardt, 1926) had the same retention time (2.0 min, Table 3-11) as that of phenyl sulfate potassium salt standard dissolved in mobile phase before HPLC analysis. No such discrepancy was observed for either chemically synthesized ß-naphthyl sulfate sodium salt or ß-naphthyl sulfate potassium salt standard when dissolved in different vehicles before HPLC analysis. The purity of both sulfate conjugates as determined by HPLC was greater than 96%, with trace amounts of N,N-diethylaniline.

Before spectrophotometric analyses, both standard and chemically synthesized sulfate conjugates were purified by solvent extraction with acetone/toluene, 1:1, solution. The phenyl sulfate infrared spectra (KBr disc) showed that the SO_3 asymmetrical stretch was found at 1280-1290 cm^{-1} and 1240-1250 cm^{-1}, SO_3 symmetrical stretch at 1060-1070 cm^{-1}, C=C-O asymmetrical stretch at 1170-1180 cm^{-1} and S-O-C stretch at

770-880 cm^{-1} (Ragan, 1978). The [^{1}H]-NMR spectrum of ß-naphthyl sulfate potassium salt standard showed a complex, asymmetric multiplet (D_2O as solvent) with major signals at 7.33, 7.43, 7.50, 7.67, 7.83, 7.93 ppm. A similar spectrum was observed for chemically synthesized ß-naphthyl sulfate sodium salt. The [^{1}H]-NMR spectra of chemically synthesized and standard phenyl sulfate also showed a complex, asymmetric multiplet (D_2O as solvent) with major signals at 7.07, 7.13, 7.17, 7.20, 7.23 ppm. Those results were comparable to those reported in literature (Ragan, 1978).

Discussion

A two-compartment pharmacokinetic model (Model A) (Figure 2-2) adequately described the plasma data after intrapericardial administration of phenol and ß-naphthol. For phenol, the half-lives for distribution and elimination phases were 8.74 ± 0.02 and 14.00 ± 0.03 min (mean ± S.D., N = 4), respectively (Table 3-6). Similar distribution phase half-life for ß-naphthol was observed for both males and females, 26 ± 19 and 29 ± 15 min, respectively, while the elimination phase half-life for males, 63.9 ± 30.9 h, was significantly longer than that of females, 30.6 ± 6.8 h (Table 3-7) ($P < 0.05$). The volume of distribution of the central compartment for phenol (204 ± 19.3 $ml \times kg^{-1}$), which includes the hemolymph, was larger than that of the peripheral compartment (145 ± 28.7 $ml \times kg^{-1}$) which indicates rapid distribution of phenol in highly perfused tissues (Table 3-6). For ß-naphthol, the volume of distribution of the central compartment (males: 297 ± 69 $ml \times kg^{-1}$; females: 342 ± 94 $ml \times kg^{-1}$) was significantly smaller

than that of the peripheral compartment (males: 561 ± 159 $ml \times kg^{-1}$; females: 776 ± 196 $ml \times kg^{-1}$) (Table 3-7) ($P < 0.05$) implying rapid distribution of ß-naphthol in the less perfused "deep" peripheral compartment.

The intercompartment (28.10 ± 2.09 $ml \times min^{-1} \times kg^{-1}$) and the whole body (28.40 ± 5.70 $ml \times min^{-1} \times kg^{-1}$) clearances of phenol (Table 3-6) indicated that the exchange of phenol between the central and peripheral compartments was as fast as the elimination of phenol from the whole animal. For ß-naphthol, the intercompartment (550 ± 530 $ml \times h^{-1} \times kg^{-1}$ for males and 500 ± 5000 $ml \times h^{-1} \times kg^{-1}$ for females) and the whole body (11.1 ± 5.9 $ml \times h^{-1} \times kg^{-1}$ for males and 26.4 ± 6.5 $ml \times h^{-1} \times kg^{-1}$ for females) clearances showed that while there was a rapid rate of exchange between the central and peripheral compartments, there was slow elimination from the whole animal. Compared to phenol, ß-naphthol had a slower rate of exchange between the central and peripheral compartments and also a slower rate of elimination from the whole animal, resulting in much longer elimination half-lives, possibly due to enterohepatic recycling of ß-naphthol and ß-naphthyl glucoside.

Phenol was cleared very rapidly from hemolymph following intrapericardial administration, and there was a quantitative dependence of dose on the route of elimination of phenol. At a low dose (0.02 mg/kg), approximately 25% of the phenol was eliminated rapidly from hemolymph into tank water, and at a higher dose (2 mg/kg), excretion into tank water predominated (see Figure 3-17). The balance of phenol at each dose level was equally rapidly eliminated from hemolymph by conjugation, primarily with sulfate (due to high K_m for phenol UDP-

glucosyltransferase, see Tables 3-1, 3-3 and 3-5), and the phenyl sulfate was slowly excreted in urine. Although this study did not directly demonstrate that the phenol excreted into tank water in the first 30 min after the dose came across the gills, gill excretion is the only feasible route of elimination of phenol into tank water. Permeation of phenol through the shell was unlikely to occur or to be unidirectional, the concentration and percentage of dose in urine at 30 min after the dose was very low (Table 3-9, Figure 3-13), and there was no evidence for fecal excretion of radioactivity. Numerous studies of other compounds with this species of lobster have demonstrated that less than 2% of the administered dose leaks from the injection site (Foureman *et al.*, 1978; Barron *et al.*, 1988; James *et al.*, 1989). Since both branchial excretion and conjugation were very rapid processes, essentially complete by 30 min after the dose, the quantitative dependence of route of excretion on dose suggested that the capacity for sulfation was saturated at a lower dose than the capacity for gill excretion.

The physico-chemical properties of phenol, a weak acid and lipophilic with log P value of 1.46, are such that branchial excretion was not unexpected, based on studies with fish (Maren *et al.*, 1968). Goth (1981) also pointed out that for lipophilic and weak acid compounds, the lipid membranes of the gills of aquatic animals offer a ready avenue for their excretion. Results from protein binding studies showed that phenol was extensively protein bound in hemolymph across a wide dose range (93.5 ± 2.5% bound), suggesting that a

facilitated excretion mechanism may be operating at the gills to remove phenol from hemolymph protein for excretion.

In comparison with phenol, ß-naphthol has a higher log P value (phenol: 1.46; ß-naphthol: 2.84) and a similar pK_a (phenol: 9.9; ß-naphthol: 9.57). From those physico-chemical properties comparisons, ß-naphthol is a better candidate than phenol for the branchial excretion. To the contrary, *in vivo* studies showed that only a small amount (1.46-14.3%) of the dose was excreted into the tank water in the first 30 min after the dose and this process was not dose dependent. The rate of branchial excretion of lobsters dosed with 0.25 mg/kg of ß-naphthol was estimated from Model B to be in the range of 10^{-5} to 10^{-6} h^{-1}, due to fast rate of sulfate and glucoside conjugations (in the range of 10^{-1} to 10^{-2} h^{-1}).

The major metabolite of phenol in the American lobster was not immediately identified as phenyl sulfate for several reasons. Firstly, the chromatographic behavior was not identical to standard phenyl sulfate unless the standard was dissolved first in a control of lobster urine (Table 3-11). Possibly the urine contains components that form ion pairs with phenyl sulfate, thereby increasing its retention time. Rhodes and Houston (1981) noted that inclusion of tetrabutylammonium salt in HPLC mobile phase altered the retention of α-naphthyl sulfate but not α-naphthyl-ß-D-glucoside. Secondly, the metabolite was somewhat resistant to acid hydrolysis, requiring 24 h in 2 N HCl before hydrolysis was complete (Figure 3-18). Sulfate esters are normally quite unstable in acid (Roy, 1981). Thirdly, the conjugate was not readily hydrolyzed by Sigma type V arylsulfatase from *Patella*

vulgata, although it was a good substrate for type VI arylsulfatase from *Aerobacter aerogenes*. The poor hydrolysis of the phenol metabolite in urine and a crude acetone extract of urine by type V arylsulfatase is probably due to the presence of other sulfate esters in lobster urine, which concentrated in the crude acetone extract and served as competitive substrates. It has been demonstrated that molluscan sulfatases are very sensitive to inhibition by substrate, whereas microbial sulfatases are insensitive (Roy, 1970). Others have documented the inhibitory effect of urine from rat (Rhodes and Houston, 1981), human and dog (Walle *et al.*, 1983) on the hydrolysis of sulfate esters by molluscan arylsulfatase. After separation of the lobster urinary metabolite from other urinary components by extraction and alumina chromatography, the metabolite was hydrolyzed completely by molluscan arylsulfatase.

Further confirmation of the identity of the phenol metabolite as phenyl sulfate was provided by comparing the positive ion FAB mass spectrum of the tetrabutylammonium ion pair of the isolated urinary metabolite with that of phenyl sulfate standard. Because phenyl sulfate was poorly soluble in glycerol and other matrices used for FAB mass spectrometry, very weak signals and high background were obtained for phenyl sulfate itself. Formation of the tetrabutylammonium ion pair of phenyl sulfate improved its solubility in glycerol and resulted in a very clean positive ion mass spectrum with *m/z* 657, due to two molecules of tetrabutylammonium cation per molecule of phenyl sulfate (Figure 3-19).

The major urinary metabolite of ß-naphthol co-migrated with ß-naphthyl-ß-D-glucoside, but was somewhat resistant to ß-glucosidase (type II from almonds) hydrolysis. Field *et al.* (1991) showed that compounds containing imidazole rings were inhibitors of ß-glucosidase type II from almonds. The lobster urine possibly contained compounds containing imidazole rings such as L-histidine which had a K_i of 7.3 μM for ß-glucosidase. The lobster urinary inhibitors were separable by HPLC from the major urinary metabolite which were not separable by Alumina N. Sep-Pak® chromatography and resulted in a metabolite fraction that was completely hydrolyzed by ß-glucosidase (7.8 units).

The time-dependent tissue distribution of [^{14}C] phenol in hemolymph and other organs showed that antennal gland had the highest concentration of [^{14}C] at 4 and 24 h after the dose, while hepatopancreas and hemolymph had similar concentrations of [^{14}C] (see Figure 3-13 and 3-14). This is contrast to findings for previously studied lipophilic xenobiotics such as benzo[a]pyrene, which concentrated in the hepatopancreas of many crustacean species (James, 1989a). *In vitro* studies showed that phenol sulfotransferase activity was present in antennal gland. From those observations, therefore, it is likely that a major site of sulfation of phenol is the antennal gland, and that the capacity for conjugation is limited by the amount of enzyme and PAPS present in the antennal gland. Only small amounts of phenyl-ß-D-glucoside were formed due to high K_m of phenol UDP-glucosyltransferase (Tables 3-3, 3-4 and 3-5). Once formed, most of the phenyl sulfate was released back into the circulating hemolymph and

only slowly excreted into urine. Excretion was especially slow in female lobsters, for as yet unknown reasons. The slow urinary excretion of phenyl sulfate was in marked contrast to the rapid elimination of the parent phenol. Thus, the usual effect of conjugation, that of facilitating excretion, was not accomplished here.

Results from HPLC analyses and enzymatic hydrolyses indicated that ß-naphthol was rapidly metabolized into sulfate and glucoside conjugates. Also, results from tissue distribution showed that antennal and hepatopancreas were organs with the highest concentrations (Figures 3-15 and 3-16). The activities of conjugating enzymes were found in both microsomal fractions of hepatopancreas and antennal gland (ß-naphthol UDP-glucosyltransferase) and cytosolic fraction of antennal gland (ß-naphthol sulfotransferase). These observations indicated that the parent compound was metabolized by the conjugating enzymes in the hepatopancreas and antennal gland to glucoside and sulfate conjugates then eliminated from the animal. Model A can not fully describe the plasma data of metabolites formed *in vivo*. Therefore, Model A was modified by inserting Michaelis-Menten elimination kinetics and become Model B which can then describe the formation and elimination of metabolites formed in the biotransformation process that took place in the American lobster.

Dedrick *et al.* (1972) used the water content of human liver to convert the unit of K_m from μM to $\mu g/ml$. Because of differences in the circulatory systems between human and lobster, the lobster conjugating enzymes, for the purpose of

the model, were considered evenly distributed in the hemolymph which was the main constituent of the central compartment. Therefore, for lobster, the volume of the central compartment was used in the conversion instead of water content of the hepatopancreas which is equivalent to the human liver. The amount of sulfate conjugate detected in hemolymph at all time points were in the range of 0.5-4% of the total radioactivity in hemolymph. As mentioned in the introduction, sulfate conjugates are substrates for sulfatases and sulfatase activity was detected in the spiny lobster. It is possible that the sulfatases are also present in the American lobster, and the rate constants of sulfatase hydrolysis are estimated from Model B to be in the range of 10^{-4} to 10^{-5} h^{-1}. The site of sulfation was antennal glands which locate next to urinary bladder (Cobb and Philips, 1980) and sulfation has been viewed as an aid to urinary excretion (Mulder, 1981). This minor conjugate, comprising 2-9.7% of the excreted [^{14}C], was formed in the antennal glands and excreted into urinary bladder, then removed from the body in the urine. The half-lives of sulfate conjugate estimated from Model B were 3.3 ± 1.6 h for males and 4.3 ± 1.7 h for females (Table 3-8) and were shorter than those of phenyl sulfate in the lobster.

Glucuronide conjugates of xenobiotics are substrates for ß-glucuronidase. In mammals, considerable ß-glucuronidase activity is present in the intestinal microflora and it can cause enterohepatic recirculation. Compounds involved in this cycle tend to have a longer half-life in the body and may undergo more extensive biotransformation before being eliminated (Sipes and Gandolfi, 1991). From the observations

that ß-naphthol and its glucoside conjugate have long elimination phase half-life and slow whole body clearances, it is proposed that this type of cycle took place in the American lobster. In the lobster, the major conjugate for ß-naphthol, glucoside conjugate, was formed in the hepatopancreas then enterohepatic recirculation occurred which was caused by the ß-glucosidase activity in the American lobster. This cycle might also contribute to the long half-life of the ß-naphthol. In Model B, k_{gn} indicated the rate constant of ß-glucosidase. The males, 0.20 ± 0.019 h^{-1}, had a higher ß-glucosidase activity than the females, 0.040 ± 0.0029 h^{-1} (Table 3-8). The long half-lives of ß-naphthyl glucoside estimated from Model B were 10.4 ± 3.7 h for females and 28.4 ± 20.6 h for males. This was possibly due to enterohepatic recirculation and high protein binding (99.7 ± 0.1% - 84.6 ± 14.3%). Another phenolic compound, α-naphthol, with similar lipophilicity, log P value of 2.98, also had a very high protein binding (92%) in the channel catfish and a three compartment model was used to describe the plasma concentration of α-naphthol with terminal phase half-lives ranging from 7.3 h at 25 mg/kg to 8.7 h at 1 mg/kg (Stehly and Plakas, 1992).

Although Model B describes the processes occurring in the lobster, the parameters did not fit the data. Model B estimated the half-life of ß-naphthyl sulfate for the males was 3.3 ± 1.6 h and 4.3 ± 1.7 h for the females, and the half-life of ß-naphthyl glucoside was 28.4 ± 20.6 h for the males and 10.4 ± 3.7 h for the females (Table 3-8). When manually estimated using a log linear plot of concentration versus time, the half-life of ß-naphthyl sulfate was 7.8 h for the

males and 9.4 h for the females and the half-life of ß-naphthyl glucoside was 51.2 h for the males and 28.9 h for the females (Table 3-8). The *in vitro* studies measured the K_m and V_{max} for ß-naphthol UDP-glucosyltransferase at 12.5°C showed that this conjugating enzyme had a lower velocity at lower temperature than at high temperature, but similar K_m. Other factors such as pH value, amount of cosubstrate in the animals also will affect the V_{max}. In *in vitro* studies, those factors were optimized. It is very likely that the values of V_{max} used in the Model B are too high. In the literature, there are very few reports showing how to convert the *in vitro* data to proper units for modeling the *in vivo* data. The conversions of the units possibly need to consider other factors, such as how the substrates are delivered to the conjugating enzymes. Further modification of the Model B is needed to get a better fit of the data.

Results from two externally cannulated female lobsters treated with 0.25 mg/kg [^{14}C]-ß-naphthol and sacrificed at 5 days showed that 13-28% of the radioactivities, including urine, were recovered, indicating that a great portion of the dose was not excreted from urine, but possibly from the gills. The parent compound was slowly eliminated from the gills as mentioned above and possibly the glucoside conjugate which was still very lipophilic also eliminated from the gills. For ß-naphthol, the major metabolite, ß-naphthyl-ß-D-glucoside, was eliminated from the animal either across the gills or in the urine.

CHAPTER 4
SUMMARY AND CONCLUSIONS

Summary

In Vitro Studies

These *in vitro* studies demonstrate that sulfotransferase and glucosyltransferase enzymes that utilize exogenous phenols as substrates are present in the American lobster, and that these enzymes are found in the hepatopancreas and antennal gland. These enzymes are comparable to those found in the vertebrate species. For substrates like phenol, sulfation may be expected to predominate when the lobster is exposed to the xenobiotic at low, environmentally relevant concentrations, whereas for substrates like ß-naphthol and 3-hydroxybenzo[a]pyrene, both sulfation and glucosidation may be expected to varying degrees. The DEAE-cellulose anion exchange chromatography suggested that there were four forms of phenol sulfotransferase in the male lobster and three in the female. The studies present indirect evidence that physiological factors related to molting may regulate the properties of sulfotransferase and possibly glucosyltransferase in the American lobster, and that multiple forms of these enzymes are present. Confirmation of both these possibilities will require further study.

In Vivo Studies

The fate of phenol in the American lobster was controlled by two competing processes, namely, excretion of parent compound into water, presumably across the gills, and biotransformation to a polar conjugate, phenyl sulfate, which was slowly excreted in urine. The contribution of each process was dose-dependent. At a dose of 25 μg/kg, branchial excretion and biotransformation occurred to equal extents, while at a dose of 2 mg/kg, branchial elimination predominated.

ß-Naphthol was rapidly metabolized by two competing conjugating enzymes, sulfotransferase (low capacity) and UDP-glucosyltransferase (high capacity) and the conjugates were slowly eliminated from the American lobster. The minor metabolite, ß-naphthyl sulfate, was formed in the antennal gland, excreted into urinary bladder, and eliminated from the body in urine. The data indicated that enterohepatic recirculation occurred for the major metabolite, the glucoside conjugate, which was formed in the hepatopancreas and the antennal gland, and slowly eliminated in urine, probably across the gills.

Conclusions

Both the *in vitro* data and the *in vivo* observations can support and explain each other. For the antennal gland sulfotransferase, there was sexual difference in handling ß-naphthol and 3-hydroxybenzo[a]pyrene, while no such difference

was observed for phenol. The antennal gland sulfotransferase had higher affinity for phenol than ß-naphthol and 3-hydroxybenzo[a]pyrene, while the hepatopancreatic UDP-glucosyltransferase handled ß-naphthol and 3-hydroxybenzo[a]pyrene better than phenol. The antennal gland UDP-glucosyltransferase handled ß-naphthol and 3-hydroxybenzo[a]pyrene better than the hepatopancreatic UDP-glucosyltransferase, but there was no such difference for phenol. The DEAE-cellulose anion exchange chromatography indicated that there were four forms of phenol sulfotransferase in male and three in female. The *in vitro* data implied that phenol was a better substrate for sulfotransferase than for UDP-glucosyltransferase and it was confirmed by the *in vivo* results which showed that the major metabolite formed *in vivo* (greater than 90%) was phenyl sulfate.

Phenol was eliminated from the lobster by two dose-dependent competing processes, excretion as parent phenol across the gills and biotransformation in the antennal gland to phenyl sulfate. The half-life of elimination of phenol from hemolymph was 14.00 ± 0.03 min and that of the phenyl sulfate 6.3 h for males and 11.9 h for females. The major route of excretion of the phenyl sulfate was through the antennal gland in urine.

ß-Naphthol was rapidly metabolized into two conjugates *in vivo*, ß-naphthyl-ß-D-glucoside (major metabolite) and ß-

naphthyl sulfate (minor metabolite). There was a sexual difference in the elimination of ß-naphthol *in vivo*. Males had a significantly longer elimination phase half-life, 63.9 ± 30.9 h, than females, 30.6 ± 6.8 h. The minor metabolite, ß-naphthyl sulfate which had a half-life of 7.8 h for the males and 9.4 h for the females, was formed in the antennal gland then excreted into urine. The major metabolite, ß-naphthyl-ß-D-glucoside, was formed in the hepatopancreas and the antennal gland and enterohepatic recirculation occurred before being eliminated from the body. The elimination half-lives of ß-naphthyl glucoside were 51.2 h for the males and 28.9 h for the females which were longer than those of ß-naphthyl sulfate.

The *in vivo* distribution of radioactivity indicated that the antennal gland was involved in the biotransformation of phenol and ß-naphthol and the hepatopancreas was only involved in the metabolism of ß-naphthol. When lipophilicity increased from log P 1.46, phenol, to log P 2.84, ß-naphthol, the elimination phase half-life increased dramatically from 14.00 ± 0.03 min to 30.6 ± 6.8 - 63.9 ± 30.9 h. From those observations, it is very likely that 3-hydroxybenzo[a]pyrene will have an even longer elimination half-life due to its higher lipophilicity, log P_{calcd} 6.34.

REFERENCES

Aiken, D.E. Proecdysis, setal development, and molt prediction in the American lobster (*Homarus americanus*). J. Fish. Res. Board Can., 30, 1337-1344, 1973.

Andersen, M.E., Clewell, H.J., Gargas, M.L., Smith, F.A. and Reitz, R.H. Physiologically based pharmacokinetics and the risk assessment process for methylene chloride. Toxicol. Appl. Pharmacol., 87, 185-205, 1987.

Anderson, R.J. and Weinshilboum, R.M. Phenolsulfotransferase in human tissue: radiochemical enzymatic assay and biochemical properties. Clinica Chimica Acta, 103, 79-90, 1980.

Banerjee, R.K. and Roy, A.B. Kinetic studies of the phenol sulphotransferase reaction. Biochim. Biophys. Acta, 151, 573-586, 1968.

Barron, M.G., Gedutis, C. and James, M.O. Pharmacokinetic of sulphadimethoxine in the lobster, *Homarus americanus*, following intrapericardial administration. Xenobiotica, 18, 269-276, 1988.

Barron, M.G., Stehly, G.R. and Hayton, W.L. Pharmacokinetic modeling in aquatic animals I. models and concepts. Aquatic Toxicol., 18, 61-86, 1990.

Bevill, R.F., Koritz, G.D., Rudawsky, G., Dittert, L.W., Huand, C.H., Hayashi, M. and Bourne, D.W.A. Disposition of sulfadimethoxine in swine: inclusion of protein binding factors in a pharmacokinetic model. J. Pharmaco. Biopharm., 10, 539-550, 1982.

Black, S.D. and Coon, M.J. P-450 cytochromes: structure and function. Adv. Enzymology, 60, 35-88, 1987.

Borchardt, R.T., Schasteen, C.S. and Wu, S.E. Phenol sulfotransferase. II. Inactivation by phenylglyoxal, N-ethylmaleimide and ribonucleotide 2',3'-dialdehydes. Biochim. Biophys. Acta, 708, 280-293, 1982.

Brown, C.A. and Black, S.D. Membrane topology of mammalian cytochrome P-450 from liver endoplasmic reticulum. J. Biol. Chem., 264, 4442-4449, 1989.

Bungay, P.M., Dedrick, R.L. and Guarino, A.M. Pharmacokinetic modeling of the dogfish shark (*Squalus acanthias*): Distribution and urinary and biliary excretion of phenol red and its glucuronide. J. Pharmacokinet. Biopharm., 4, 377-388, 1976.

Burchell, B. and Coughtrie, M.W.H. UDP-glucuronosyltransferases. Pharmacol. Ther., 43, 271-289, 1989.

Burchell, B., Nebert, D.W., Nelson, D.R., Bock, K.W., Iyanagi, T., Jansen, P.L.M., Lancet, D., Mulder, G.J., Chowdhury, J.Y., Siest, G., Tephly, T.R. and Mackenzie, P.I. The UDP glucuronosyltransferase gene superfamily: suggested nomenclature based on evolutionary divergence. DNA and cell biology, 10, 487-494, 1991.

Burkhardt, G.N. and Lapworth, A. Arylsulphuric acids. J. Chem. Soc., 684-690, 1926.

Campbell, N.R., Van Loon, J.A. and Weinshilboum, R.M. Human liver phenol sulfotransferase: assay conditions, biochemical properties and partial purification of isoenzymes of the thermostable form. Biochem. Pharmacol., 36, 1435-1446, 1987.

Capel, D., French, M.R., Millburn, P., Smith, R.L. and Williams, R.T. The fate of [^{14}C]-phenol in various species. Xenobiotica, 2, 25-34, 1972.

Chen, L.J. Bile salt sulfotransferase in guinea pig liver. Biochim. Biophys. Acta, 717, 316-321, 1982.

Clarke, D.J., George, S.G. and Burchell, B. Glucuronidation in fish. Aquat. Toxicol., 20, 35-56, 1991.

Clewell, H.J. and Andersen, M.E. Risk assessment extrapolations and physiological modeling. Toxiol. Ind. Health, 1, 111-131, 1985.

Cobb, J.S. and Phillips, B.F. The biology and management of lobsters. Volume I, Academic Press, New York, 1980.

Comer, K.A. and Falany, C.N. Immunological characterization of dehydroepiandrosterone sulfotransferase from human liver and adrenal. Mol. Pharmacol., 41, 645-651, 1992.

Dedrick, R.L., Forrester, D.D. and Ho, D.H.W. *In vitro - in vivo* correlation of drug metabolism-deamination of 1-ß-D-arabinofuranosylcytosine. Biochem. Pharmacol., 21, 1-16, 1972.

Dooley, T.P., Walker, C.J., Hirshey, S.J., Falany, C.N. and Diani, A.R. Localization of minoxidil sulfotransferase in rat liver and the outer root sheath of anagen pelage and vibrissa follicles. J. Invest. Dermatol., 96, 65-70, 1991.

Duffel, M.W., Binder, T.P. and Rao, S.I. Assay of purified aryl sulfotransferase suitable for reactions yielding unstable sulfuric acid esters. Anal. Biochem., 183, 320-324, 1989.

Duffel, M.W., Binder, T.P., Hosie, L., Baden, H.A., Sanders, J.A., Knapp S.A. and Baron J. Purification, immunochemical characterization, and immunohistochemical localization of rat hepatic aryl sulfotransferase IV. Mol. Pharmacol., 40, 36-44, 1991.

Dutton, G.J. Glucuronidation of drugs and other compounds. CRC Press, Boca Raton, Fl, 1980.

Elmamlouk, T.H. and Gessner, T. Carbohydrate and sulfate conjugations of p-nitrophenol by hepatopancreas of Homarus americanus. Comp. Biochem. Physiol., 61C, 363-367, 1978.

Falany, C.N. Molecular enzymology of human liver cytosolic sulfotransferase. Trends in Pharmacol. Sci., 12, 255-259, 1991.

Falany, C.N. and Tephly, T.R. Separation, purification and characterization of three isoenzymes of UDP-glucuronyl-transferase from rat liver microsomes. Arch. Biochem. Biophys., 227, 248-258, 1983.

Falany, C.N., Vazquez, M.E., Heroux, J.A. and Roth, J.A. Purification and characterization of human liver phenol-sulfating phenol sulfotransferase. Arch. Biochem. Biophys., 278, 312-318, 1990.

Field, R.A., Haines, A.H., Chrystal, E.J.T. and Luszniak, M.C. Histidines, histamines and imidazoles as glycosidase inhibitors. Biochem. J., 274, 885-889, 1991.

Foldes, A. and Meek, J.L. Rat brain phenolsulfotransferase-partial purification and some properties. Biochim. Biophys. Acta, 327, 365-374, 1973.

Foureman, G.L., Zvi, B-Z., Dostal, L., Fouts, J.R. and Bend, J.R. Distribution of ^{14}C-benzo(a)pyrene in the lobster at various times after a single injection into the pericardial sinus. Bulletin of the Mount Desert Island Biological Laboratory, 18, 93-95, 1978.

Fry, J.R. and Paterson, P. Influence of lipid solubility on the glucuronidation and sulphation of nitrophenols in rat isolated hepatocytes. Br. J. Pharmacol., 84, 133P, 1985.

Gerlowski, L.F. and Jahn, R.K. Physiologically based pharmacokinetic modeling: principles and applications. J. Pharm. Sci., 72, 1103-1126, 1983.

Gibaldi, M. Biopharmaceutics and clinical pharmacokinetics. Fourth edition, Lea & Febiger, Philadelphia, 1991.

Gibaldi, M. and Perrier, D. Pharmacokinetics. Second edition, Marcel Dekker Inc., New York, 1982.

Gilbert, E.E. Sulfonation and Related Reactions, Interscience, New York, 1965.

Goksøyr, A. and Förlin, L. The cytochrome P-450 system in fish, aquatic toxicology and environmental monitoring. Aquat. Toxicol., 22, 287-312, 1992.

Gorge, G., Beyer, J. and Urich, K. Excretion and metabolism of phenol, 4-nitrophenol and 2-methylphenol by the frogs, *Rana temporia* and *Xenopus laevis*. Xenobiotica, 17, 1293-1298, 1987.

Goth, A. Medical pharmacology. Tenth edition, The C.V. Mosby company, St. Louis, 1981.

Hernandez, J.S., Watson, R.W.G. Wood, T.C. and Weinshilboum R.M. Sulfation of estrone and 17 ß-estradiol in human liver, Catalysis by thermostable phenol sulfotransferase and by dehydroepiandrosterone sulfotransferase. Drug Metab. Dispos., 20, 413-422, 1992.

Heroux, J.A. and Roth, J.A. Physical characterization of a monoamine-sulfating form of phenol sulfotransferase from human platelets. Mol. Pharmacol., 34, 194-199, 1988.

Himmelstein, K.J. and Lutz, R.J. A review of the application of physiologically based pharmacokinetic modeling. J. Pharmacokinet. Biopharm., 7, 127-145, 1979.

Hirshey, S.J., Dooley, T.P., Reardon, I.M., Heinrikson, R.L. and Falany, C.N. Sequence analysis, *in vitro* translation, and expression of the cDNA for rat minoxidil sulfotransferase. Mol. Pharmacol., 42, 257-264, 1992.

Holliday, C.W. A new method for measuring the urinary rate of a brachyuran crab. Comp. Biochem. Physiol., 58A, 119-120, 1977.

James, M.O. Catalytic properties of cytochrome P-450 in hepatopancreas of the spiny lobster, *Panulirus argus*. Marine Environmental Research, 14, 1-11, 1984.

James, M.O. Xenobiotic conjugation in fish and other aquatic species. In "Xenobiotic Conjugation Chemistry" (Menn, J.J., Caldwell, J., Hutson, D. and Paulsen, G. edited). American Chemical Society Symposium Series. No. 299, 29-47, 1986.

James, M.O. Conjugation of organic xenobiotics in aquatic animals. Env. Hlth. Persp., 71, 97-103, 1987.

James, M.O. Biotransformation and disposition of PAH in aquatic invertebrates. In "Metabolism Polycyclic Hydrocarbons in the Aquatic Environment" (Varanasi U. edited), 69-91. CRC Press, Boca Raton, Fl, 1989a.

James, M.O. Conjugation and excretion of xenobiotics by fish and aquatic invertebrates. In "Xenobiotic metabolism and disposition" (Kato, R., Estabrook, R.W. and Cayen, M.N. edited). Taylor & Francis Ltd., 283-290, 1989b.

James, M.O. Cytochrome P450 monooxygenases in crustaceans. Xenobiotica, 19, 1063-1076, 1989c.

James, M.O. Isolation of cytochrome P450 from hepatopancreas microsomes of the spiny lobster, *Panulirus argus*, and determination of catalytic activity with NADPH cytochrome P450 reductase from vertebrate liver. Arch. Biochem. Biophys., 282, 8-17, 1990.

James, M.O., Barron, M.G. and Schell, J.D. Conjugation and excretion of phenolic compounds by the lobsters, *Homarus americanus*. Bulletin of the Mount Desert Island Biological Laboratory, 27, 9-11, 1987.

James, M.O. and Little, P.J. Characterization of cytochrome P-450 dependent mixed-function oxidation in spiny lobster, *Panulirus argus*. In "Developments in Biochemistry: Biochemistry, Biophysics and Regulation of Cytochrome P-450" (Gustafsson, J.A. edited), Elseriver/North Holland Biomedical Press, Amsterdam, 13, 113-120, 1980.

James, M.O. and Little, P.J. 3-Methylcholanthrene does not induce *in vitro* xenobiotic metabolism in spiny lobster hepatopancreas, or affect *in vivo* disposition of benzo(a)pyrene. Comp. Biochem. Physiol., 78C, 241-245, 1984.

James, M.O., Schell, J.D. and Magee, V. Bioavailability biotransformation and elimination of benzo(a)pyrene-7,8-dihydrodiol in the lobster, *Homarus americanus*. Bulletin of the Mount Desert Island Biological Laboratory, 28, 119-121, 1989.

James, M.O., Schell, J.D. Barron, M.G. and Li, C.L.J. Rapid, dose-dependent elimination of phenol across the gills, and slow elimination of phenyl sulfate in the urine of phenol-dosed lobsters, *Homarus americanus*. Drug Metab. Dispos., 19, 536-542, 1991.

James, M.O., Sherman, B., Fisher, S.A. and Bend, J.R. Benzo[a]pyrene metabolism in reconstituted monooxygenase systems containing cytochrome P-450 from lobster (*Homarus americanus*) hepatopancreas fractions and NADPH-cytochrome P-450 reductase from pig liver. Bulletin of the Mount Desert Island Biological Laboratory, 22, 37-39, 1982.

James, M.O., Warner, M. Serabjit-Singh, C., and Bend, J.R. Cytochrome P450 dependent mixed function oxidation in the spiny lobster. Federation Proceedings, 38, 443, 1979.

Johannes, A., Meyerinck, L.V. and Schmoldt, A. Purification of rat liver cytosolic sulfotransferase responsible for the conjugation of digitoxigenin. Biochem. Pharmacol., 39, 301-309, 1990.

Johnson, J. J. and Corbett, M.D. The uptake and *in vivo* metabolism of the organophosphate insecticide Fenitrothion by the blue crab, *Callinectes sapidus*. Toxicol. Appl. Pharmacol., 85, 181-188, 1986.

Karara, A.H. and Hayton, W.L. Pharmacokinetic model for the uptake and disposition of di-2-ethylhexyl phthalate in sheephead minnow (*Cyprinodon variegatus*). Aquat. Toxicol., 5, 181-195, 1984.

Kauffman, F.C., Whittaker, M., Anundi, I. and Thurman, R.D. Futile cycling of a sulfate conjugate by isolated hepatocytes. Mol. Pharmacol., 39, 414-420, 1991.

King, F.G., Dedrick, R.L. Collins, J.M. Matthews, H.B. and Birnbanum, L.S. Physiological model for the pharmacokinetics of 2,3,7,8-tetrachlorodibenzofuran in several species. Toxicol. Appl. Pharmacol., 67, 390-400, 1983.

Klaassen, C.D. and Rozman, K. Absorption, distribution and excretion of toxicants. In "Casarett and Doull's Toxicology" (Amdur, M.O., Doull, J. and Klaassen, C.D. edited), fourth edition, Pergamon Press, New York, 50-87, 1991.

Laemmli, U.K. Cleavage of structural proteins during the assembly of the head of bacteriophage T4. Nature (London), 227, 680-685, 1970.

Layiwola, P.J. and Linnecar, D.F.C. The biotransformation of [^{14}C]-phenol in some freshwater fish. Xenobiotica, 11, 167-171, 1981.

Leo, A., Hansch, C. and Elkins, D. Partition coefficients and their uses. Chem. Rev., 71, 525-616, 1971.

Lotlikar, P.D., Scribner, J.D., Miller, J.A. and Miller, E.C. Reactions of esters of aromatic N-hydroxyamines and amides with methionine *in vitro*: a model for *in vivo* binding of amine carcinogens to protein. Life Sci., 5, 1263-1269, 1966.

Low, L.K. and Castagnoli, N. Jr. Metabolic changes of drugs and related organic compounds. In "Wilson and Gisvold's Textbook of Organic Medicinal and Pharmaceutical Chemistry" (Doerge, R.F. edited), eighth edition, J.B. Lippincott, Philadelphia, 55-127, 1982.

Lowry, O.H., Rosebrough, N.J., Farr, A.L. and Randall, R.J. Protein measurement with Folin phenol reagent. J. Biol. Chem., 193, 265-275, 1951.

Lutz, R.J. Dedrick, R.L. Tuly, D., Sipes, I.G., Anderson, M.W. and Matthews, H.B. Comparison of the pharmacokinetics of several polychlorinated biphenyls in mouse, rat, dog, and monkey by means of a physiological pharmacokinetic model. Drug Metab. Dispos., 12, 527-535, 1984.

Malins, D.C. and Ostrander, G.K. Perspectives in aquatic toxicology. Annu. Rev. Pharmacol. Toxicol., 31, 371-399, 1991.

Maren, T.H., Embry, R. and Broder, L.E. The excretion of drugs across the gill of the dogfish, *Squalus acanthias*. Comp. Biochem. Physiol., 26, 853-864, 1968.

Maziasz, T.J., Liu, J., Madhu, C. and Klaassen, C.D. The differential effects of hepatotoxicants on the sulfation pathways in rats. Toxicol. Appl. Pharmacol., 110, 365-373, 1991.

Miller, J.J., Powell, G.M., Olavesen, A.H. and Curtis, C.G.: The fate of 2,6-dimethoxy[U-^{14}C]phenol in the rat. Xenobiotica, 4, 285-289, 1974.

Miranda, C.L., Wang, J.L., Henderson, M.C. and Buhler, D.R. Purification and characterization of hepatic steroid hydroxylases from untreated rainbow trout. Arch. Biochem. Biophys., 268, 227-238, 1989.

Morello, A. and Repetto, Y. UDP-glucosyltransferase activity of housefly microsomal fraction. Biochem. J., 177, 809-812, 1979.

Mulder G.J. Sulfation of Drugs and Related Compounds. CRC Press, Boca Raton, Fl, 1981.

Mulder, G.J. Conjugation of phenols. In "Metabolic Basis of Detoxication" (Jakoby, W.B., Bend, J.R. and Caldwell, J. edited). Academic Press, 248-270, 1982.

Mulder G.J. Conjugation reactions in drug metabolism. Taylor & Francis Ltd., 1990.

Nebert, D.W., Nelson, D.R., Coon, M.J., Estabrook, R.W., Feyereisen, R., Fujii-Kuriyama, Y., Gonzalez, F.J., Guengerich, F.P., Gunsalus, I.C., Johnson, E.F., Loper, J.C., Sato, R., Waterman, M.R. and Waxman, D.J. The P450 superfamily: update on new sequences, gene mapping, and recommended nomenclature. DNA and cell biology, 10, 1-14, 1991.

Nichols, J.W., McKim, J.M., Lien, G.J., Hoffman, A.D. and Bertelsen, S.L. Physiologically based toxicokinetic modeling of three waterborne chloroethanes in rainbow trout (*Oncorhynchus mykiss*). Toxicol. Appl. Pharmacol., 110, 374-389, 1991.

Nichols, J.W., McKim, J.M., Andersen, M.E., Gargas, M.L., Clewell III, H.J. and Erickson, R.J. A physiologically based toxicokinetic model for the uptake and disposition of waterborne organic chemicals in fish. Toxicol. Appl. Pharmacol., 106, 433-447, 1990.

Niehrs, C. and Huttner, W.B. Purification and characterization of tyroylprotein sulfotransferase. The EMBO Journal, 9, 35-42, 1990.

Nose, Y. and Lipmann, F. Separation of steroid sulfokinases. J. Biol. Chem., 233, 1348-1351, 1958.

Ogura, K., Sohtome, T., Sugiyama, A., Okuda, H., Hiratsuka, A. and Watabe, T. Rat liver cytosolic hydroxysteroid sulfotransferase (sulfotransferase a) catalyzing the formation of reactive sulfate esters from carcinogenic polycyclic hydroxymethylarenes. Mol. Pharmacol., 37, 848-854, 1990.

Orrenius, S., Anderson, B., Jernström, B. and Moldeus, P. Isolated hepatocytes as an experimental tool in the study of drug conjugation reactions. In "Conjugation Reactions in Drug Biotransformation" (Aitio, A. edited). Elsevier/North Holland Publishing, Amsterdam, 273, 1978.

Ragan, M.A. Phenol sulfate esters: ultraviolet, infrared, [^{1}H] and [^{13}C] nuclear magnetic resonance spectroscopic investigation. Can. J. Chem., 56, 2681-2685, 1978.

Ramsey, J.C. and Andersen, M.E. A physiologically based description of the inhalation pharmacokinetics of styrene in rats and humans. Toxicol. Appl. Pharmacol., 73, 159-175, 1984.

Real, M.D. and Ferré, J. Biosynthesis of Xanthurenic acid 8-O-ß-D-glucoside in *Drosophila*. Characterization of the xanthurenic acid: UDP-glucosyltransferase activity. J. Biol. Chem., 265, 7407-7412, 1990.

Real, M.D., Ferré, J. and Chapa, F.J. UDP-glucosyltransferase activity toward exogenous substrates in *Drosophila melanogaster*. Anal. Biochem., 194, 349-52, 1991.

Rhodes, J.C. and Houston, J.B. Quantification of naphthyl conjugates. Comparison of high-performance liquid chromatography and selective enzymes hydrolysis methods. Xenobiotica, 11, 63-70, 1981.

Rowland, M. Physiologic pharmacokinetic models and interanimal species scaling. Pharmacol. Ther., 29, 49-68, 1985.

Roy, A.B. The hydrolysis of sulfate esters. In "The Enzymes", Vol. V, 1-20, Academic Press, New York, 1970.

Roy, A.B. Sulfotransferases. In "Sulfation of Drugs and Related Compounds" (Mulder, G.J. edited), 83-130, CRC Press, Boca Raton, Fl, 1981.

Rozman, P., Kim, H.J., Madhu, C., Gregus, Z. and Klaassen, C.D. Homeostasis of sulfate and 3'-phosphoadenosine 5'-phosphosulfate in rats with deficient dietary intake of sulfur. Drug Metab. Dispos., 20, No. 3, 374-378, 1992.

Sanborn H.R. and Malins, D.M. The disposition of aromatic hydrocarbons in adult spot shrimp (*Pandalus platyceros*) and the formation of metabolites of naphthalene in adult and larval spot shrimp. Xenobiotica, 10, 193- 200, 1980.

Schell, J.D. and James, M.O. Glucose and sulfate conjugation of phenolic compounds by the spiny lobster, *Panulirus argus*. J. Biochem. Toxicol., 4, 133-138, 1989.

Sekura, R.D. and Jakoby, W.B. Phenol sulfotransferases. J. Biol. Chem., 254, 5658-5663, 1979.

Sekura, R.D., Marcus, C.J., Lyon, E.S. and Jakoby, W.B. Assay of sulfotransferase. Anal. Biochem., 95, 82-85, 1979.

Sindermann, C.J. Pollution-associated diseases and abnormalities of fish and shellfish: A review. Fish. Bull., 76, 717-749, 1979.

Sipes, I.G. and Gandolfi, A.J. Biotransformation of toxicant, In "Casarett and Doull's Toxicology" (Amdur, M.O., Doull, J. and Klaassen, C.D. edited), fourth edition, Pergamon Press, New York, 88-126, 1991.

Smith, G.E. and Griffiths, L.A. Comparative metabolic studies of phenacetin and structurally-related compounds in the rat. Xenobiotica, 6, 217-236, 1976.

Snyder, M.J. and Chang, E.S. Metabolism and excretion of injected [^{3}H]-ecdysone by female lobsters, *Homarus americanus*. Biol. Bull., 180, 475-484, 1991.

Stegeman, J.J. Polynuclear aromatic hydrocarbons and their metabolism in the marine environment. In "Polycyclic hydrocarbons and Cancer" (Gelboin, H.V. and Ts'O, P.O.P. edited), Academic Press, New York, 1981.

Stehly, G.R. and Hayton, W.L. Disposition of pentachlorophenol in rainbow trout (*Salmo gairdneri*): effect of inhibition of metabolism. Aquat. Toxicol., 14, 131-148, 1989.

Stehly, G.R. and Plakas, S.M. Disposition of 1-naphthol in the channel catfish (*Ictalurus punctatus*). Drug Metab. Dispos., 20, 70-73, 1992.

U.S. Department of Commerce Statistical Abstract of the United States 1992. 112th Edition, 1992.

Vanstapel, F. and Blanckaert, N. Endogenous esterification of bilirubin by liver microsomes. J. Biol. Chem., 262, 4616-4623, 1987.

Walle, T., Walle, U.K., Knapp, D.R., Conradi, E.C. and Bargar, E.M. Identification of major sulfate conjugates in the metabolism of propranolol in dog and human. Drug Metab. Dispos., 11, 344-349, 1983.

Wheldrake, J.F., Baudinette, R.V. and Hewitt, S. The metabolism of phenol in a desert rodent *Notomys alexis*. Comp. Biochem. Physiol., 61C, 103-107, 1978.

White, R.E. and Coon, M.J. Oxygen activation by cytochrome P-450. Ann. Rev. Biochem., 49, 315-356, 1980.

Williams, D.E. and Buhler, D.R. Benzo[a]pyrene-hydroxylase catalyzed by purified isozymes of cytochrome P-450 from ß-naphthoflavone-fed rainbow trout. Biochem. Pharmacol., 33, 3743-3753, 1984.

Williams, R.T. Detoxification mechanisms, ed. 2, Wiley, New York, 1959.

Winsnes, A. Kinetic properties of different forms of hepatic UDP-glucuronyltransferase. Biochim. Biophys. Acta, 284, 394-405, 1972.

Zaharko, D.S., Dedrick, R.L. and Oliverio, V.T. Prediction of the distribution of methotrexate in the sting rays *Dasyatidae sabina* and *sayi* by use of a model developed in mice. Comp. Biochem. Physiol., A42, 183-194, 1972.

BIOGRAPHICAL SKETCH

Chung-Li Jason Li was born on October 28, 1960, in Hsinchu, Taiwan. He was graduated from Cheng-Kung High School, Taipei, Taiwan, in 1979 and matriculated in the Taipei Medical College, Taipei, Taiwan, in 1980 where he earned a Bachelor of Science degree in pharmacy. Following graduation in 1984, he served in the China Army as a medical doctor. He retired from the Army in 1986 and immigrated to the United Stated in 1987. He entered the University of Florida in 1988 as a graduate student in the Department of Medicinal Chemistry and joined the research group of Dr. M.O. James at the same year.

On September 21, 1990, he married Chi-Yin Gina Wu and their first baby, a girl, Catherine Y.F. Li, was born on November 9, 1992.

His scientific interests include the drug metabolism and pharmacokinetics of environmental pollutants in different animal species including aquatic species, and factors affecting the sulfate and carbohydrate conjugating enzymes in the American lobster.

I certify that I have read this study and that in my opinion it conforms to acceptable standards of scholarly presentation and is fully adequate, in scope and quality, as a dissertation for the degree of Doctor of Philosophy.

Margaret O. James, Chair
Professor of Medicinal Chemistry

I certify that I have read this study and that in my opinion it conforms to acceptable standards of scholarly presentation and is fully adequate, in scope and quality, as a dissertation for the degree of Doctor of Philosophy.

Raymond J. Bergeron
Professor of Medicinal Chemistry

I certify that I have read this study and that in my opinion it conforms to acceptable standards of scholarly presentation and is fully adequate, in scope and quality, as a dissertation for the degree of Doctor of Philosophy.

William R. Kem
Professor of Pharmacology and Therapeutics

I certify that I have read this study and that in my opinion it conforms to acceptable standards of scholarly presentation and is fully adequate, in scope and quality, as a dissertation for the degree of Doctor of Philosophy.

Kenneth B. Sloan
Associate Professor of Medicinal Chemistry

This dissertation was submitted to the Graduate Faculty of the College of Pharmacy and to the Graduate School and was accepted as partial fulfillment of the requirements for the degree of Doctor of Philosophy.

August, 1993

Dean, College of Pharmacy

Dean, Graduate School